CSDL-R-1901

PERFORMANCE & APPLICATIONS OF A HYBRID JET SELECTION & CMG STEERING LAW BASED ON LINEAR PROGRAMMING

by

Joseph A. Paradiso

October 1986

The Charles Stark Draper Laboratory, Inc.
555 Technology Square
Cambridge, Massachusetts 02139

CSDL-R-1901

Performance and Applications of a Hybrid Jet Selection and CMG Steering Law Based on Linear Programming

by

Joseph A. Paradiso

October, 1986

ABSTRACT

Linear programming techniques have been applied to develop a CMG steering law which exhibits very high adaptability to CMG hardware failures and variations in CMG system definition. The procedure is also capable of performing a fuel-optimal jet selection and establishing control via a hybrid mixture of jets and CMGs. This report summarizes the results of simulations that have been performed to examine the capabilities and advantages of the resulting hybrid selection/steering procedure.

INTRODUCTION

Space station attitude control will most likely be provided by Control Moment Gyros (CMGs), while momentum desaturation and translational control will be accomplished through Reaction Control System (RCS) jets and/or environmental torques. Previous spacecraft control systems have managed such dissimilar sets of actuators via independent control laws linked only through operational requirements.

The anticipated mission requirements on a space station place a high premium on reliability and efficiency. To meet these demands, it is highly desirable to develop control laws which are able to derive maximum benefit from both types of actuators (CMGs and jets), used independently and in coordinated combination. Examples of the latter include use of jets to augment the response of a degraded CMG system (i.e., CMGs unable to deliver desired torque or momentum due to hardware failure), attitude maneuvers requiring large rates, simultaneous attitude and position control, and simultaneous maneuvering and momentum desaturation.

A further consideration is the requirement to control across significant vehicle configuration changes occurring during build-up, docking, and articulation. The space station mass properties and actuator configuration/response will evolve substantially during these operations, requiring a capability to track such changes and accommodate them in the control system. While desensitizing the control system may be adequate for stability purposes, high reliability and efficiency require an adaptive actuator management and control strategy.

Existing CMG control and steering systems are generally subject to drawbacks and restrictions which can prove significantly disadvantageous for space station operation. Particular mounting orientations and specific modes of CMG usage are often implicit in the structure of most CMG steering laws[1]. Hardware saturation (i.e., peak limits on CMG output torque and stop constraints on gimbal excursion) is not considered in most CMG steering procedures, thus must be

enforced after the CMG selection has been performed. These limitations can appreciably compromise the flexibility and accuracy of available CMG response.

The effort summarized in this report has addressed these challenges, and has resulted in an efficient and extremely flexible actuator management procedure which can be used to steer a CMG system, perform fuel-optimal jet selections, and control spacecraft via a hybrid mixture of jets and CMGs. Prototype controllers and vehicle simulations have also been developed to examine the performance and features of this novel approach to actuator selection and steering.

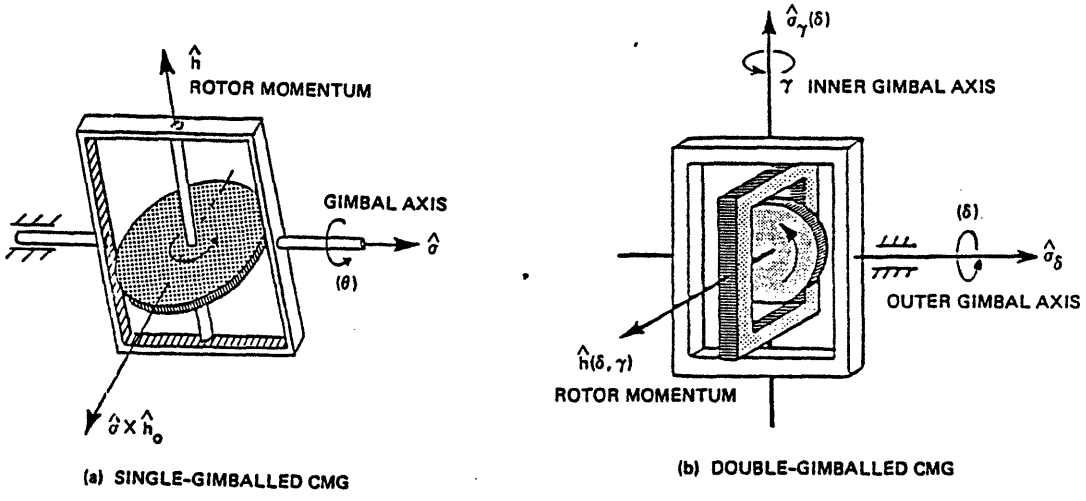

FIGURE 1: SINGLE AND DOUBLE GIMBALLED CMGs

APPROACH

The original approach taken to develop the hybrid actuator selection process has been summarized in Reference 2 and detailed in Reference 3. The current structure of the steering/selection procedure is qualitatively described below.

CMGs are momentum exchange devices which create an output torque by changing the orientation of angular momentum stored in a rotor spinning at constant rate. The two standard CMG types are depicted in Fig. 1. Figure 1a shows a single gimballed CMG (rotor constrained to

gimbal in a fixed plane), and Figure 1b shows a double gimballed CMG (rotor able to align with any direction given sufficient gimbal freedom). The angular velocity of each CMG gimbal may be commanded to yield an output torque, which is instantaneously described by the vector product of gimbal rate and corresponding rotor momentum.

The hybrid selection process optimally commands an array of CMGs to produce either a vehicle torque or change in vehicle angular rate. A Linear programming algorithm is used to calculate a set of gimbal displacements in response to a commanded rate change (in the latter case, CMG gimbal rates are normalized such that the gimbal which moves the farthest is run at its peak rate).

The instantaneous output torque of each CMG gimbal is used to form a set of "activity vectors" for linear programming selection. CMG systems generally possess more available degrees of freedom than required for control purposes, thus often admit several possible solutions. The linear programming process converges to the particular solution which meets the input command while minimizing an objective function that penalizes CMG configurations of low controllability, thereby encouraging avoidance of problematic CMG orientations. The objective calculation for double gimballed CMG's includes terms which act to avoid parallel and antiparallel rotor alignment (which can lead to singular CMG orientations and degraded control capability), encourage inner gimbal angles to be kept minimal (large inner gimbal angles reduce the control authority of the outer gimbal), and remove CMGs from the vicinity of gimbal stops. Since singular states of a single gimballed CMG ensemble are not always related to rotor alignment, they are instead steered to directly maximize 3-axis control authority; anti-singularity objective factors are derived from a matrix of CMG output torque vectors representing net system controllability[4].

Each CMG gimbal may be moved in two directions (i.e., "forward" and "backward" rotation), corresponding to positive and negative CMG gimbal rates and/or displacements. Linear programs, however, do not normally admit solutions containing negative decision variables; the structure of the selection algorithm was thus modified to enable specification of "bipolar" CMG gimbal motion, as detailed in Reference 3. Two objective coefficients are calculated per CMG gimbal, representing the consequence of gimbal rotation in the respective sense. Under the net objective minimization, gimbals are encouraged to move in the directions that avoid configurational difficulty as outlined above.

The "upper bound simplex" algorithm[5] has been adapted to perform linear CMG selection. When solving for CMG gimbal displacements in response to an input rate-change request, the simplex process incorporates upper bounds on the decision variable, which, in this case, represent restrictions on CMG travel imposed by gimbal stops. These bounds are also made to decrease as the CMG system approaches momentum saturation, thereby directly accounting for the reduced CMG control capacity.

When solving for CMG gimbal rates in response to an input torque request, the simplex upper bounds directly limit the decision variables such that peak gimbal rates are not exceeded. When a gimbal stop is approached, the corresponding upper bound is decreased to account for the limited travel available in that direction.

Solutions derived via conventional linear programming (without upper bounds) contain only as many non-zero decision variables as there are dimensions in the control request (i.e., only 3 CMG gimbals will be specified in the response to a 3-axis request), which does not generally yield an appropriate means of commanding a multi-CMG system. Adoption of upper bounds remedies this difficulty; solutions derived via upper bound simplex contain as many CMG gimbals as required to "optimally" answer the input request. If the request is too large (or CMGs are approaching saturation), the upper-bound simplex solution will contain "artificial variables", which indicate that the CMGs are unable

to provide the requested output, and suggests the introduction of jets (possessing higher control authority), or application of an alternate strategy, as detailed below.

Because the expression used to form activity vectors is an instantaneous approximation to the CMG output torque, the linear CMG selection must be iterated periodically with updated activity vectors and objective coefficients (all CMG controllers run in this fashion; to maintain a constant torque as the CMGs rotate, the CMG gimbal rates must be periodically re-calculated). The CMG control software used to produce the test results presented in this report allows the CMGs to rotate no further than five degrees before forcing an update selection.

A method of reducing this nonlinear "crosscoupling" effect has been developed to improve the accuracy of linear CMG solutions to rate-change requests. The exact momentum transfer resulting from the set of gimbal displacements specified by the simplex solution is calculated via a simple vector sum weighted by sines and cosines of the gimbal angles involved[6]. If this actual momentum transfer is found to differ appreciably from that requested, simplex may be re-invoked to solve for the momentum residual, and gimbal displacements from both solutions may be superimposed to form a substantially more accurate CMG response.

Linear programming has been used to perform highly adaptable, fuel-optimal jet selections in the Draper-developed OEX advanced autopilot[7], which has been successfully flight-tested[8] onboard the Shuttle Orbiter. This capability has been retained in the hybrid control package. Activity vectors representing jets are derived from jet thrusts and placements (both translational and rotational components are calculated; jet activity vectors are 6-dimensional quantities). The simplex selection process determines a set of jet firing times in response to an input rate-change request. In order to converge to a minimum-burn, fuel-optimal solution, objective factors for jets are made proportional to their fuel usage rate.

Provided that the input torque or rate change is within the capabilities of the current CMG configuration and not large enough to

drive the CMG system into saturation, the linear program is performed with jets inhibited, and simplex will produce an exclusively CMG-based solution. If the request is too large or the CMG array has neared saturation, the linear program will indicate that the desired output cannot be realized solely with CMGs. The ability of an arbitrary CMG array to produce a given rate change may also be quantitatively determined by the value of a "saturation index", which defines the ratio of the desired final CMG momentum state to the largest possible projection of CMG momentum in the final state direction (formulating the saturation index for a CMG system including single gimballed devices required the development of special projection formulae, as documented in Ref. 3). If this ratio is greater than unity, the CMGs will be driven into saturation by the input request.

If the input request cannot be realized with CMGs alone (as defined via the above conditions), a "hybrid" selection may be performed in which both sets of actuators are made available for selection, yielding simultaneous CMG displacements and jet on-times in response to an input vehicle rate-change request. The balance of jet vs CMG usage in hybrid selections is governed by both the mean CMG-to-jet objective factor ratio and the CMG upper bound values. Under the current convention, hybrid selections are generally performed with reduced CMG upper bounds in order to realize the bulk of the maneuver with jets and preserve CMGs for rotational trimming (thereby avoiding lengthy maneuver durations and saturated CMGs). Jet costs are made compatible with mean CMG costs during hybrid selections in order to favor "cheaper" CMG activity vectors which correspond to CMG motion in the most favorable directions. Such hybrid selections thus often tend to "desaturate" the CMG array, and remove it from problematic orientations.

The simplex selection is capable of solving a six-component input request, thereby providing coordinated control of vehicle translation and rotation. Hybrid selections made for such cases employ jets to achieve the desired translational impulse and introduce CMGs to aid in rotational stability.

The linear programming selection package is capable of coordinating actuators under several different modes of operation. CMGs may be selected exclusively in answer to either input rate-change or torque requests. Jets may be commanded exclusively in response to input rate changes. Jets and CMGs may be handled independently (i.e., jets produce a requested rate-change, while CMGs are simultaneously instructed to generate a torque); this mode is useful in desaturating the CMGs or damping extraneous vehicle rates created by quantized jet firings. Finally, jet and CMG activity may be coordinated under a hybrid selection, as discussed above. The latter feature is a unique application of the linear programming selection scheme.

Conventional CMG steering laws require the addition of an independent "null motion" procedure to continuously calculate gimbal rates which redistribute the CMGs into more controllable orientations without transferring momentum to the host vehicle (torque-producing gimbal rates, as calculated in conventional steering laws, tend to lead the CMGs into singular orientations). When steering via linear programming, this is achieved via the objective function; objective minimization encourages the CMGs to avoid singular orientations as they respond to input commands, thus no additional null rates are required. The ability to redistribute the CMGs without torquing the vehicle may, however, prove to be desirable; i.e., in cases where the CMGs are to be restored from an initial sub-optimal orientation. The simplex selection is able to calculate null rates with very little modification; by allowing objective factors to become negative and zeroing the input request, null gimbal rates are directly produced. The amount of "null" gimbal redistribution present in the CMG response to requests of finite magnitude may be increased by allowing the objective factors to also become negative when performing conventional selections.

If jets and CMGs are selected together during the null motion process, coordinated jet firings and gimbal motion will be specified such that the net CMG system cost is reduced, thereby moving the CMGs away from problematic orientations and momentum saturation (as

reflected in the CMG objective factors), hence achieving a "desaturation" effect while holding constant vehicle rates. Jet desaturation may also be performed in a more conventional manner by firing jets to transfer momentum into the spacecraft along the saturation axis while simultaneously commanding the CMGs to produce a compensating torque in the opposite direction.

In summary, the application of linear programming to CMG selection has produced an extremely flexible CMG steering law. Activity vectors representing linearized actuator response are kept in a common pool which is scanned during each simplex selection. Actuator failures may be accommodated by preventing corresponding activity vectors from being selected by the simplex process (and eliminating the failed devices from the objective calculations). Since each CMG gimbal is modeled via an independent activity vector, single gimbals of dual-gimballed CMGs may be failed (i.e., frozen at constant position), still leaving the surviving gimbal available for selection. Gimbal stops and peak gimbal rates are represented by bounds imposed by simplex on selected gimbal rates and displacements; these are considered directly in each simplex selection, and may be inserted, removed, or re-defined at any time. Actuator response and vehicle mass properties are represented by parameters used in activity vector calculation which may be easily changed and updated. Since specific CMG mounting configurations are not assumed anywhere in the selection process, CMGs may be mounted in any orientation. A linearized objective function is optimized in each selection, eliminating the need of a separate "null motion" procedure to calculate gimbal rates which avoid problematic CMG orientations. Null motion, if desired, may also be calculated directly under simplex by requesting a zero net rate change using a modified objective function. The same linear programming procedure is able to perform fuel-optimal jet selections and simultaneously command CMGs and jets in a coordinated fashion. Jets may be used to desaturate the CMG array under null motion or by commanding both actuators independently to transfer opposing momentum impulses.

FIGURE 2: PARALLEL MOUNTED CMG CONFIGURATION

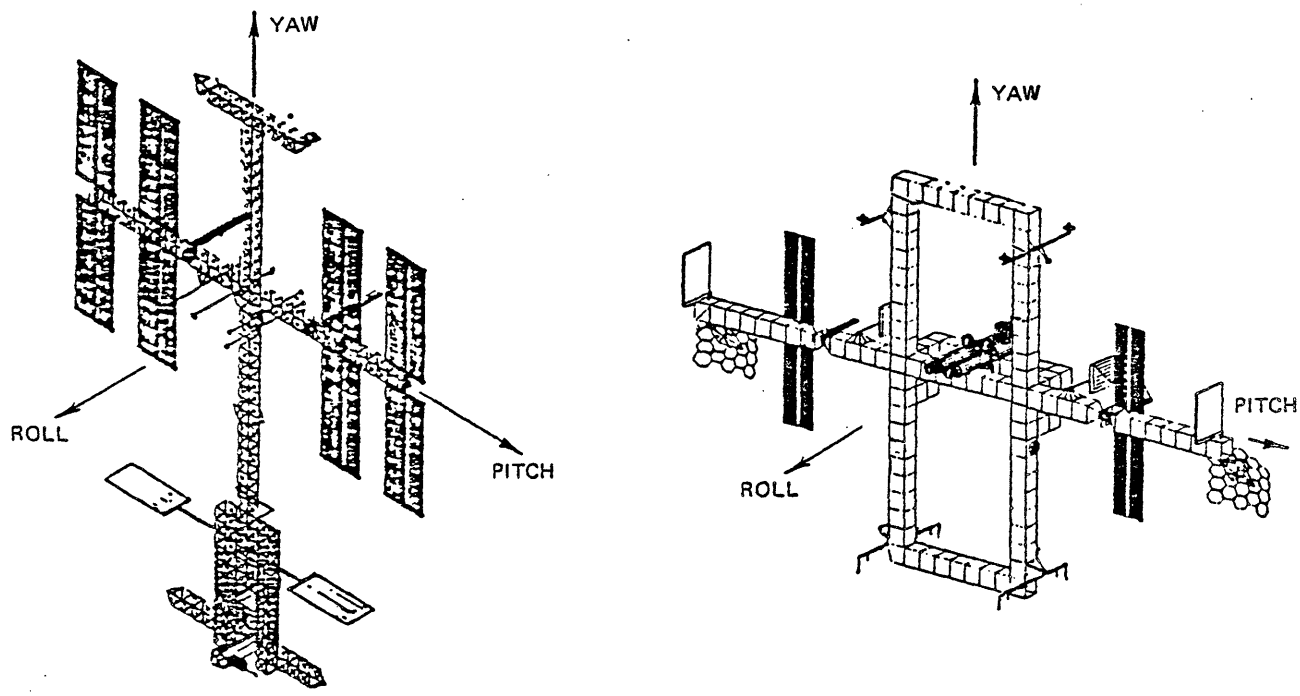

POWER TOWER SPACE STATION

Dual-keel Space Station

(a) SPACE STATION REFERENCE CONFIGURATIONS

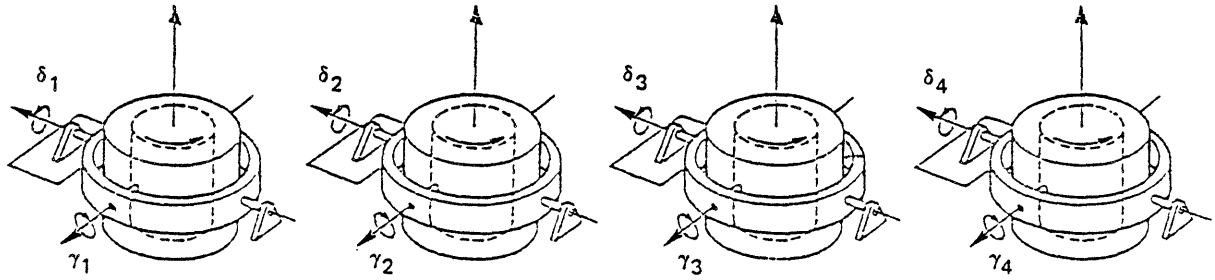

(b) PARALLEL MOUNTED CMG REFERENCE CONFIGURATION (ZERO GIMBAL ANGLES)

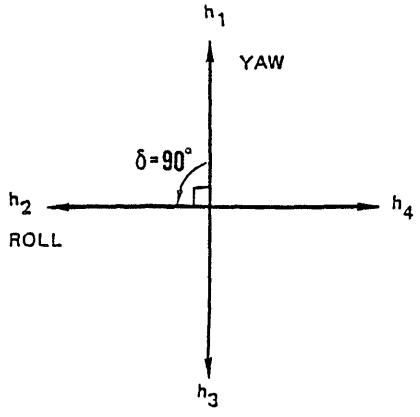

(c) INITIAL ORIENTATION OF CMG ROTORS

This method of linear programming selection is not necessarily limited to jets and CMGs; other devices (such as reaction wheels) can potentially be included, provided that they may be effectively represented by linearized activity vectors, objective coefficients, and upper bounds.

SIMULATION RESULTS

a) Simulation Setup and Conventions

In order to test the performance of the hybrid selection/steering procedure, it has been interfaced to a closed-loop control system based upon the OEX Advanced Autopilot[7]. This autopilot incorporates a phase-space control law, which derives vehicle rate-change commands

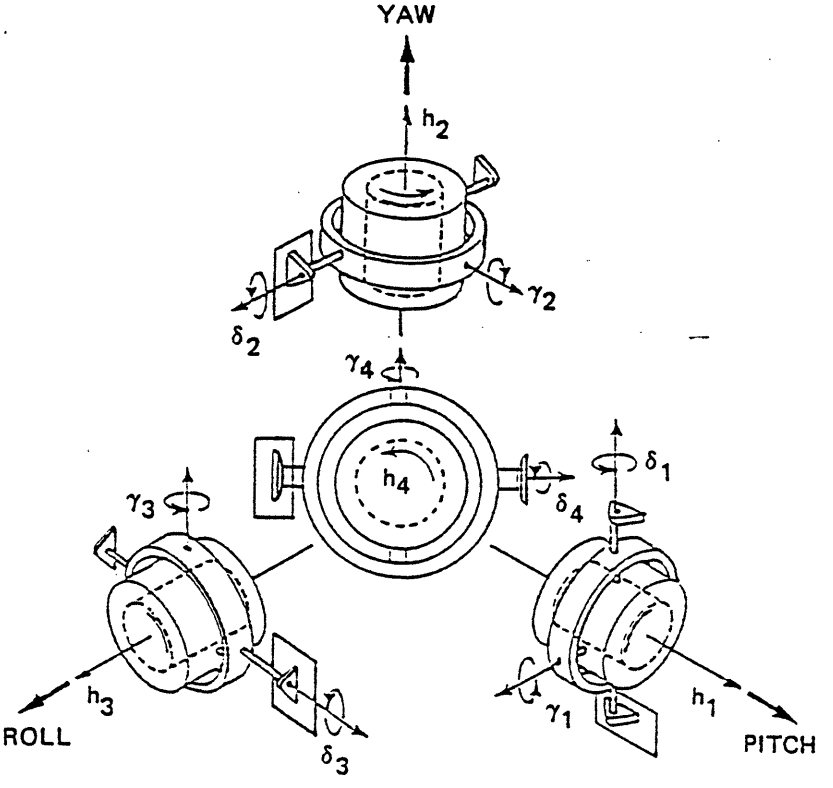

INITIAL CMG ORIENTATION

FIGURE 3: ORTHOGONAL MOUNTED CMG CONFIGURATION

from a weighted sum of vehicle attitude and rate errors, providing coordinated control of vehicle rotational states. Mass properties of the Power Tower[9] and Dual Keel[10] Space Stations (without orbiter attached) have been used in these simulations (see Figure 2a). Double gimballed CMGs are assumed mounted in either of two standard arrangements (it is possible to define any mounting protocol with this steering law). Figure 2b illustrates the "parallel" mounting configuration (assumed by most control laws proposed for the space station; e.g., Ref. 1), where all CMGs are mounted with outer gimbal axes parallel. This configuration is initialized in a "T" orientation, with all inner gimbals at zero displacement and outer gimbals initially spaced uniformly apart such that all rotors are symmetrically oriented, and the net CMG momentum sums to zero (as depicted in Figure 2c for a system of 4 CMGs). The other standard double gimballed CMG mounting setup, termed "orthogonal mounting", is depicted in Figure 3, which shows the CMGs in their initial orientation. This mounting style was derived from the convention used in Skylab[11] (three CMGs initially perpendicular), with a fourth added skewed at equal angles to each of the others. When orthogonal arrays contain over four CMGs, the additional devices are skew-mounted in the other quadrants.

All CMGs are modeled in accordance with recent specifications proposed for the space station[12]; i.e., an angular momentum capacity of 3500 ft-lb-s per rotor, and peak gimbal rates of 5 deg/s on both inner and outer gimbals. Stops are imposed at +/-90 degs. on inner gimbal travel, and the outer gimbal is assumed capable of continuous 360-degree rotation. "Ideal" CMGs are assumed in the simulation, and higher-order dynamic effects (e.g., gimbal acceleration torques, servo effects, etc.) are not currently included.

The standard arrangement assumed for single gimballed CMGs is termed "pyramid" mounting, where CMG rotors gimbal in planes which form

the faces of a regular pyramid, as depicted in Figure 4 for a 5-CMG array. Single gimballed CMGs are modeled with a limit of +/-180° on gimbal rotation. Other parameters (peak rate, etc.) are identical to those defined above for double gimballed devices.

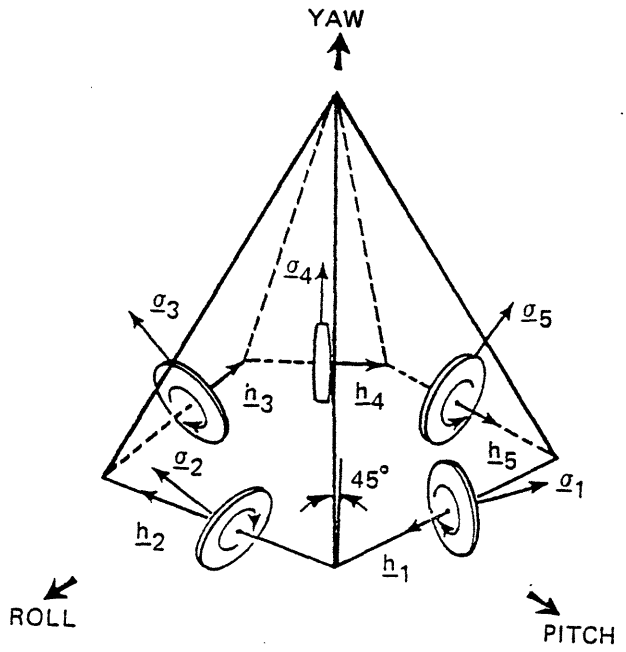

FIGURE 4: PYRAMID MOUNTED SINGLE GIMBALLED CMG CONFIGURATION

All space station models are assumed to possess 12 RCS jets, which operate at a nominal thrust of either 75 lb (Power Tower) or 10 lb (Dual Keel) each, and are clustered into planar triads located at four positions on the spacecraft (see Reference 3). While holding LVLH attitude, all jets are oriented in the orbital plane; no direct out-of-plane thrust is possible with this configuration. Jets are assumed to be discrete devices, and firings are rounded to the closest 80 ms increment. No separate logic is used to introduce jets; they are prescribed and selected by simplex as discussed in the previous section.

b) Verification of Features and Performance

The set of tests presented below consists of a series of sequenced maneuver commands performed under various conditions in order to demonstrate the capabilities and features of the linear programming approach to CMG/RCS management. All examples in this section are performed in an inertial environment; Euler coupling and precessional torques due to rotation of stored CMG momentum are included as disturbances, while aerodynamic and gravity gradient torques, which would be present on-orbit, are ignored. Vehicle rates are initialized to zero at the start of each test.

Example #1: Validation of Objective Function

As mentioned earlier, the objective function is used to steer the CMGs away from problematic orientations (i.e., rotor alignments and excessive inner gimbal angles). The first example in this series demonstrates how the anti-alignment and inner gimbal minimization contributions affect CMG steering.

A Power Tower model is assumed, driven by an array of 4 orthogonally-mounted CMGs (Figure 3). A series of rate increases (0.003 deg/s each) are commanded about the vehicle's pitch and roll axes (the yaw rate is held at zero). Five such increases are requested, building net rates of 0.015 deg/s over the 100 s duration of the test run. This is a significant rate, considering the sizable vehicle inertias ($10^6 \rightarrow 10^7$ slug-ft^2) and limited CMG control authority. Two test cases are considered; one with a complete objective function, and another without including the anti-lineup component.

Gimbal angles for both cases are shown in Figure 5. Results using a complete objective are shown in the left column; both inner and outer gimbal systems are seen to be employed in answering requests (excessive inner gimbal swings are avoided), and jets are required to complete maneuvers (as indicated by asterisks) toward the end of the

run. The results for the test omitting the anti-lineup component are shown in the right column. The remaining objective components work only to minimize the inner gimbal angles, and this is indeed what is noted in Figure 5c; the inner gimbals are hardly used until they are required to complete requests at the conclusion of the test.

CMG rotor alignments are portrayed in the upper portion of Figure 6. The complements of the relative angles between all possible CMG rotor pairs are plotted (there are 6 combinations of pairs possible in a 4-CMG system). A parallel lineup is indicated when a curve nears +90°, an antiparallel lineup is indicated when a curve nears -90°, and the respective CMG rotors are orthogonal (the "ideal" case) when the curve is in proximity to zero. When using the complete objective function (Figure 6a), CMGs are generally seen to avoid alignment until all move together toward saturation at the close of the test. When lineup avoidance is not considered in the objective (Figure 6b), CMG rotors are seen to more frequently approach alignment; at the positions indicated on the plot, rotor pairs moved within 10° of parallel and antiparallel alignment before saturation was reached. The extreme minimization of inner gimbal angles attained in this case was performed at the expense of avoiding interim CMG rotor alignments. In both test cases, jets were automatically selected by simplex when continued CMG performance was inhibited due to momentum saturation.

Vehicle rates are plotted in the lower portion of Figure 6. The commanded input about the pitch and roll axes is plotted as the dotted "staircase"; the vehicle rates (solid lines) are seen to follow this input. Since rotor alignments are avoided, the average CMG control authority is generally higher, and a quicker vehicle response is noted in the run incorporating the complete objective function. The last requested rate increase occurs after the CMGs have reached momentum saturation, hence it is answered primarily via an RCS response; due to their greater control authority, the vehicle is seen to respond more rapidly when jets are employed. The vehicle maintains a constant yaw attitude while rates are commanded around the other axes. Although a small yaw disturbance is encountered when jets participate in maneuvers

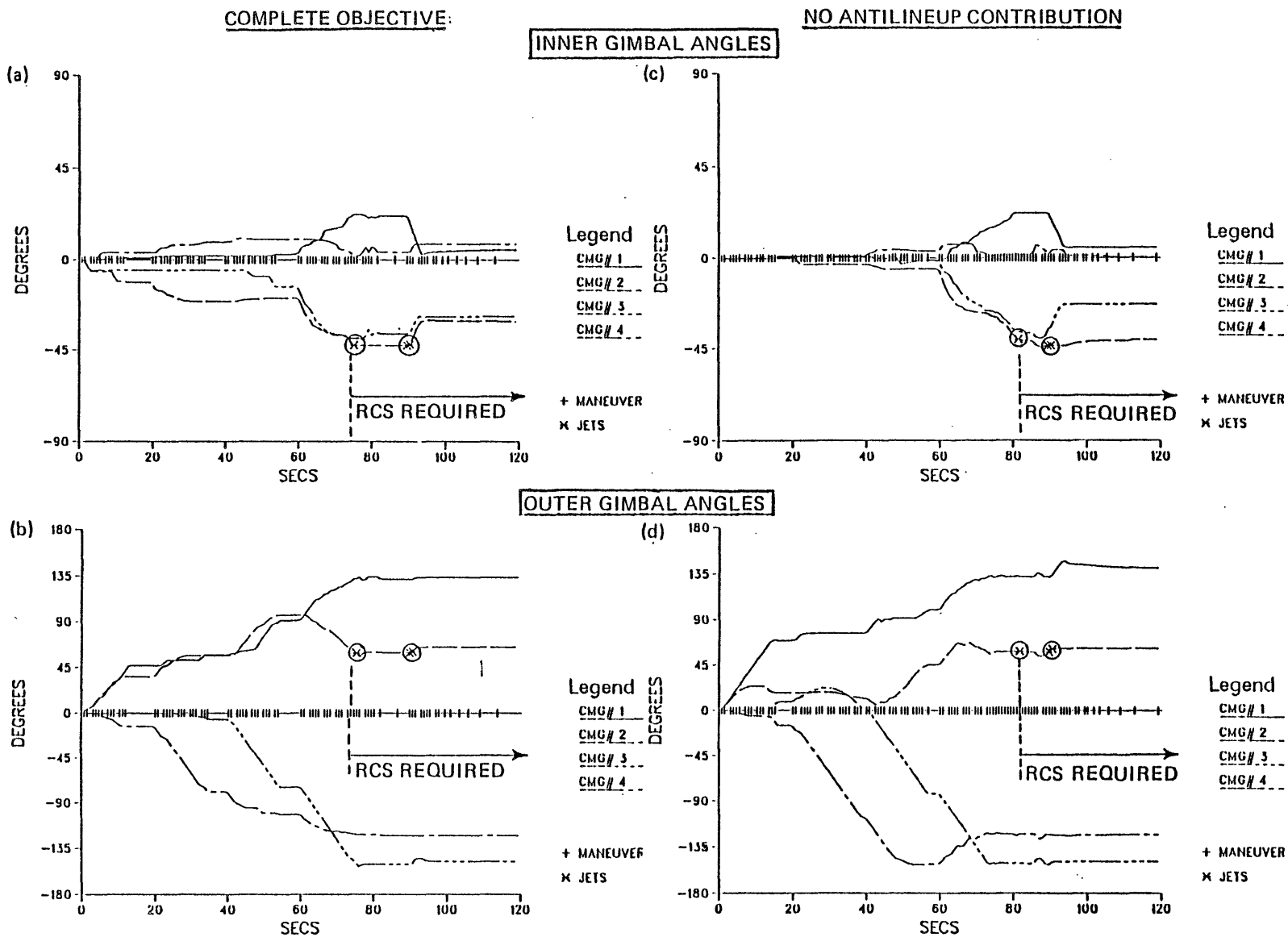

FIGURE 5: HYBRID RESPONSE TO CMG SATURATION

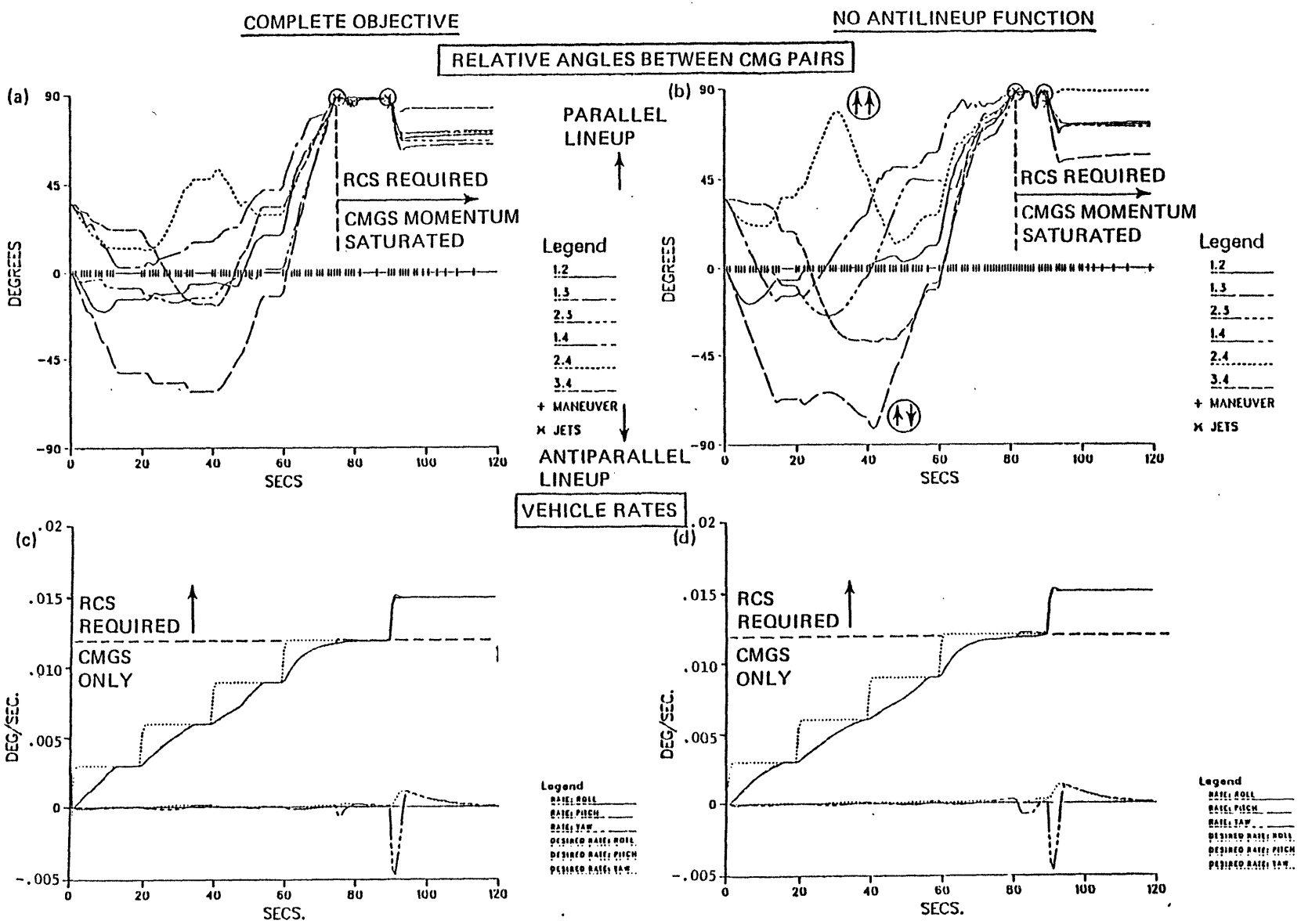

FIGURE 6: HYBRID RESPONSE TO CMG SATURATION

(the moment of inertia is an order of magnitude smaller in this coordinate), it is easily compensated by the phase space controller.

Example #2: Automatic Jet Response and Single Gimbal Failures

A major advantage of steering CMGs via linear programming is the ease with which the system of available actuators may be dynamically reconfigured and re-defined. Linear programming also provides a unique ability to blend jets and CMGs under a single selection procedure; jets are automatically introduced in response to commands which exceed available CMG control authority. The next example demonstrates these abilities; a mixed jet/CMG response is required when an excessive vehicle rate increment is commanded, and the CMG ensemble is instantly reconfigured into a single gimballed system when all outer gimbals are failed.

This example also assumes the Power Tower model, but uses an orthogonally-mounted 5-CMG array; four are included as depicted in Figure 3, and a fifth "skewed" CMG is added perpendicular to CMG #4. The command sequence consists of two rate-change requests followed by attitude holds. The initial segment requests 0.03 deg/s about the pitch axis, and enters attitude hold after 30 s have elapsed. Once the vehicle rates have settled and the desired attitude has been acquired, a rate of 0.005 deg/s is requested about the roll axis. All CMG outer gimbals are failed after this rate is achieved; thus subsequent CMG control must be realized exclusively with inner gimbals. After keeping this rate for approx. 60 s, an attitude hold is commanded, and rates are again brought to zero.

Results are given in Figure 7. Gimbal angles are plotted in the left column; note that jets were introduced to establish and remove the commanded 0.03 deg/s pitch rate. Since the CMG array (as mounted and initialized in this configuration) can only provide enough momentum to achieve approx. 0.015 deg/s along this axis, jets are required to reach the desired value of 0.03 deg/s. Because of the restrictive upper bounds placed upon CMG gimbal displacement in solutions including jets (as described earlier), CMG participation is limited in responding to

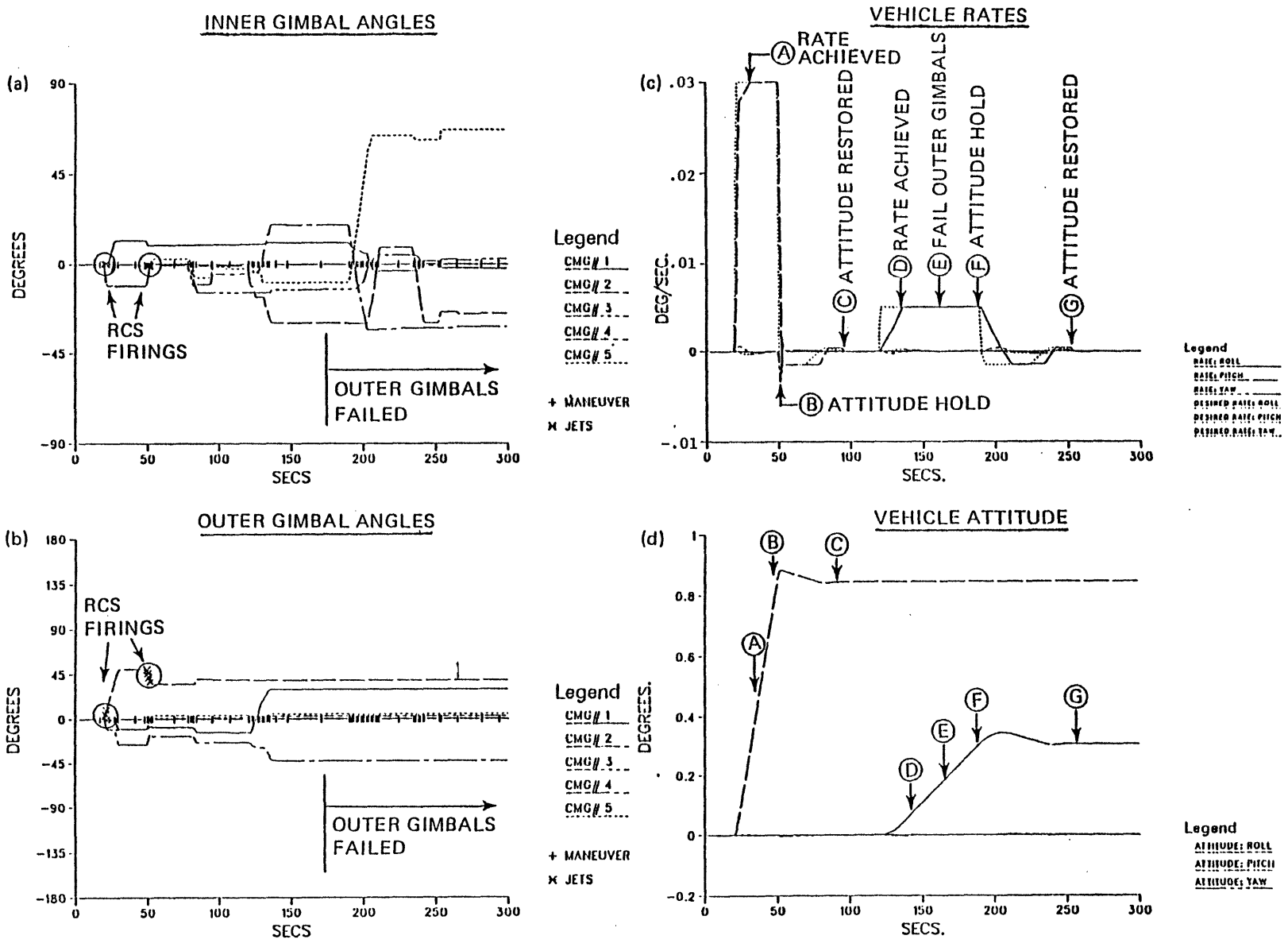

FIGURE 7: HYBRID RESPONSE TO LARGE REQUESTS AND GIMBAL FAILURES

this request, and the bulk of maneuvering is accomplished via the jets. This prevents the CMGs from being first driven into saturation before introducing jets; the hybrid response to such a large input request favors a jet-based solution in order that the CMGs are not saturated when the final state is achieved.

Vehicle rates are given in Figure 7c. The 0.03 deg/s request is seen to be quickly established (A) and removed (B) primarily via jets. The attitude hold is commanded while the vehicle is coasting at 0.03 deg/s. There is no feedforward implementation of attitude commands; instructions are executed by the controller as they arrive. Because of this, the vehicle is made to coast at approximately -0.002 deg/s after the attitude hold is commanded in order to compensate for attitude errors accumulated during deceleration. This rate is removed and the vehicle is stabilized (C) entirely via the CMG system (0.002 deg/s is well within the CMG control margin).

After vehicle rates have damped to zero, a 0.005 deg/s rate is requested about the roll axis. This is handled exclusively by the CMGs, and no jets are required (see Figs. 7a and b). After this rate is achieved (D), the outer gimbals of all CMGs are failed (i.e., frozen at constant position and inhibited from selection {E}), and an attitude hold is commanded (F). As seen in Figs. 7a and b, this was achieved entirely via the inner gimbal system; no RCS assistance was required. At point G, vehicle attitude was restored, and rates were returned to zero.

Vehicle attitudes are plotted in Figure 7d. The command sequence executed in this test established attitude changes of approximately 0.85 deg. in pitch and 0.3 deg. in roll. Yaw attitude remains at zero, as commanded.

Even though the CMG selection process can instantly adapt to commanding single gimballed CMGs, effective singularity avoidance in such a CMG system cannot be achieved by merely steering away from rotor alignments; modifications to the objective which address this problem are outlined and demonstrated in Example 7.

Example #3: Adaptation to Changing Vehicle Mass Properties

Since the vehicle mass properties are incorporated into the calculation of actuator activity vectors, the selection process is easily able to adapt to a changing vehicle configuration. This ability is demonstrated in the following test, which initially assumes the mass properties of the Dual Keel Space Station (approximately 2.5 times heavier than the Power Tower), controlled by six double gimballed CMGs mounted in the orthogonal configuration (i.e., Figure 3). Two identical maneuver sequences are commanded. Each sequence begins by requesting a rate of 0.0008 deg/s along the vehicle pitch axis. This rate is held after it is achieved, and an attitude hold is commanded after 50 s have elapsed since the start of the maneuver. The vehicle inertia about the pitch axis is decreased by 50% before the second maneuver begins.

Resulting vehicle rates are plotted in the lower portion of Figure 8. The desired peak rates are attained and removed; the feedback controller creates the small undershoots at the close of each maneuver in order to restore vehicle attitude following receipt of the attitude hold instruction. We see a somewhat faster, yet nearly identical vehicle response when the pitch inertia is reduced, indicating that the controller was able to adapt to the change in vehicle environment without difficulty.

The corresponding CMG gimbal activity is illustrated in the plot of outer gimbal angles presented in the upper portion of Fig. 8 (inner gimbal angles were kept minimal by the objective function). Because the vehicle responds more promptly to CMG motion after the inertia reduction, the CMGs are seen to follow somewhat different trajectories when answering each set of commands.

Example #4: Introduction of Jets After CMG Failures

In the event of hardware failures severe enough to prevent the CMGs from answering input commands, the hybrid selection has the

COMMAND 2 STEPS IN PITCH; VEHICLE INERTIA CHANGE

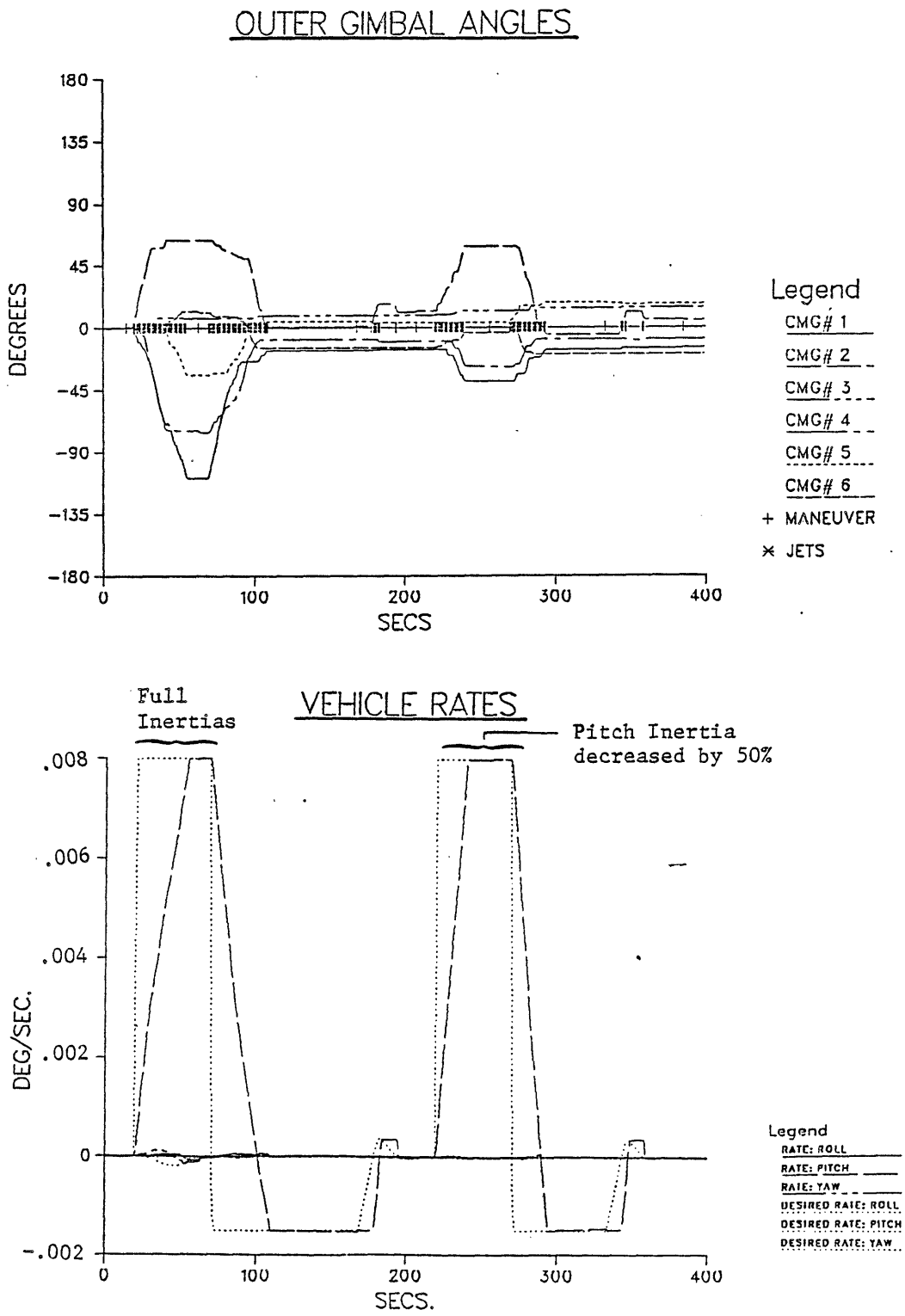

FIGURE 8

COMMAND 2 STEPS IN PITCH; FAIL CMGS 1 AND 2

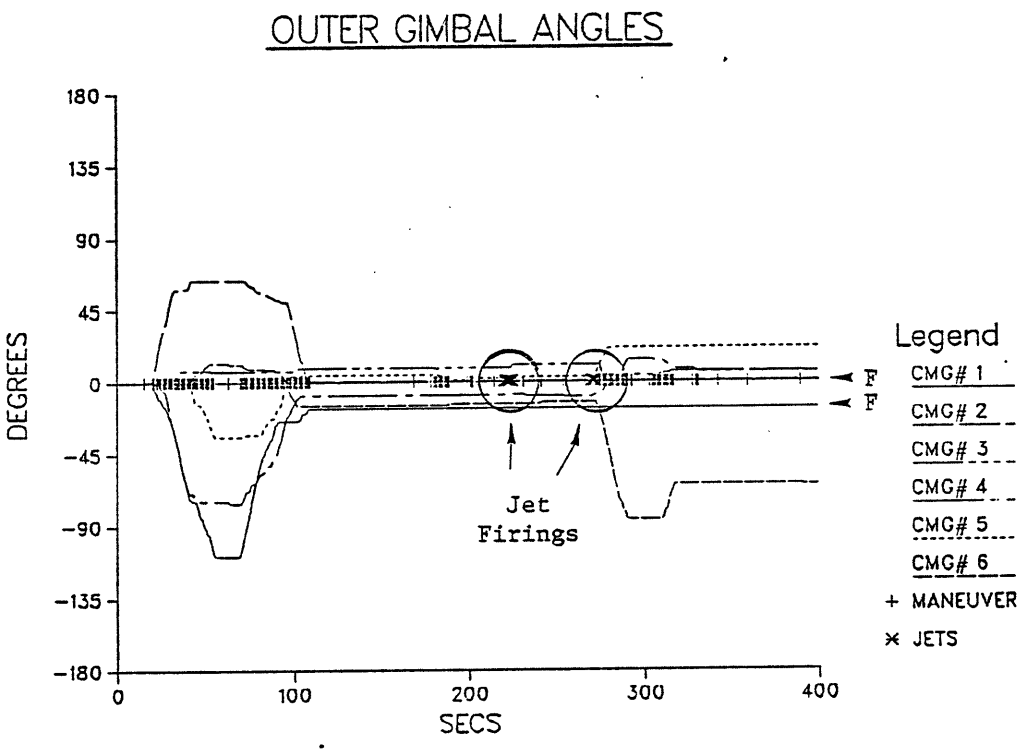

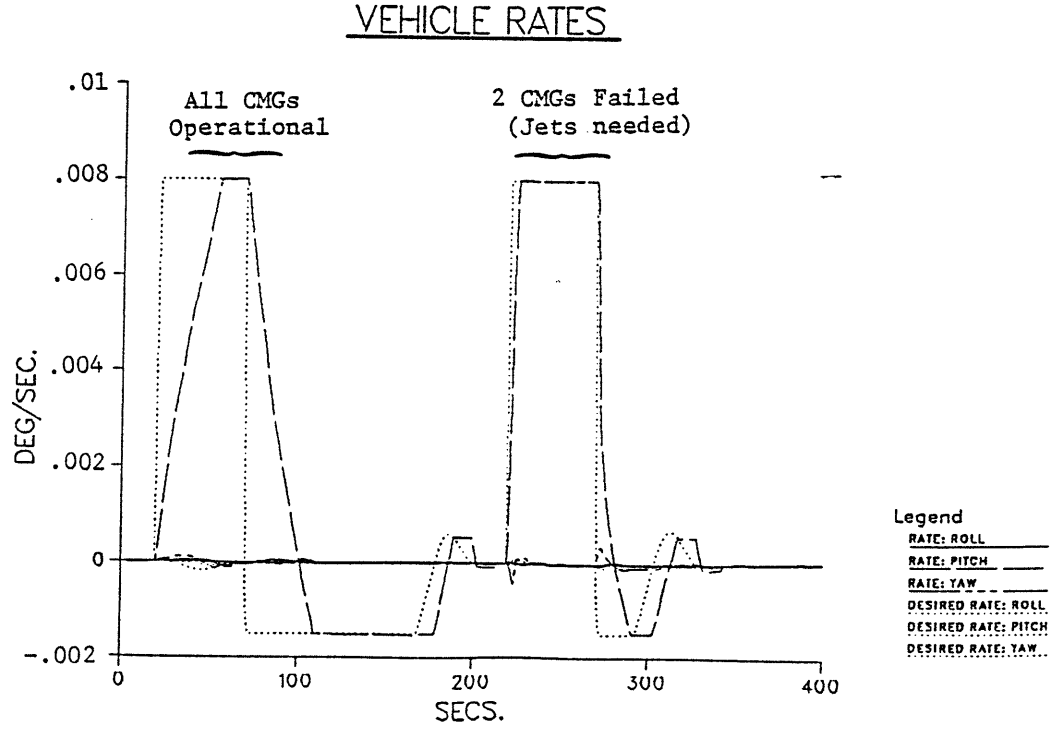

FIGURE 9

ability to automatically introduce jets in order to recover the needed control authority. This is illustrated in the next test, which assumes an identical setup (6 ortho-mounted CMGs driving the Dual Keel), and uses an identical input command sequence (two 0.008 deg/s rate commands followed by attitude holds). The first set of commands is again implemented nominally. Two CMGs are failed (i.e., inhibited from selection) before the second set begins.

Outer gimbal angles and vehicle rates are plotted in Fig. 9. Because of the limited control authority available from the truncated CMG configuration, the rate increase and decrease cannot be attained solely by the CMGs, hence the bulk of the second command sequence is handled primarily via jet firings (which yield much greater torque, hence cause considerably faster vehicle response). CMGs are still used exclusively to damp vehicle rates and restore attitude, and the controller has encountered no difficulty in achieving the desired vehicle response using the truncated CMG system together with reaction control jets.

Example #5: Dynamic Redefinition of Gimbal Stops

Most CMG steering laws are incapable of accounting for restrictions on gimbal freedom (i.e., gimbal stops), which must usually be imposed in an "ad hoc" fashion after gimbal rates are calculated. The linear programming approach accounts for gimbal stops both in the objective function (i.e., encouraging CMGs not to closely approach stops) and directly as upper bounds on the decision variables (i.e., forcing the selection to limit the corresponding gimbal rotation). The location of gimbal stops is specified as a parameter in the selection software, and thus may be dynamically redefined at will (i.e., if a CMG gimbal is degraded, the selection can prevent its rotation past an arbitrarily defined angle).

The test run of Figure 10 illustrates how gimbal stops may be easily altered under the linear programming approach. A Dual Keel model is assumed to be driven by an array of six parallel-mounted CMGs

FIGURE 10: Dynamic Definition of CMG Gimbal Stops

No Stops on Outer Gimbal

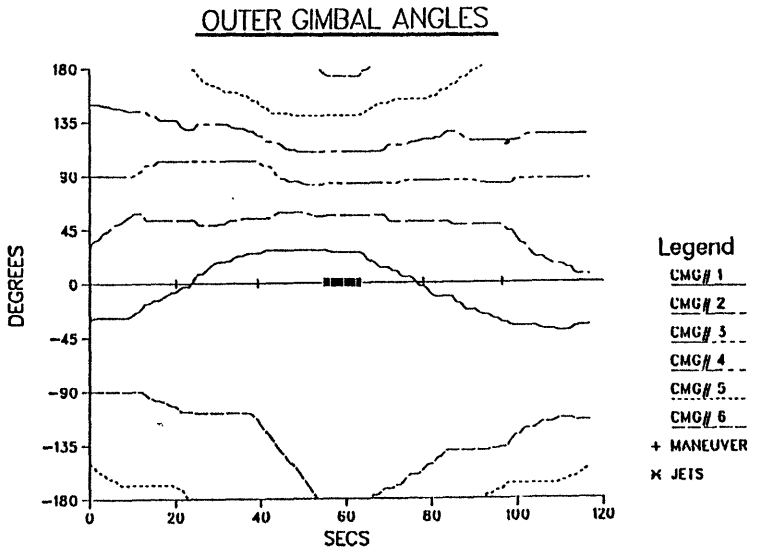

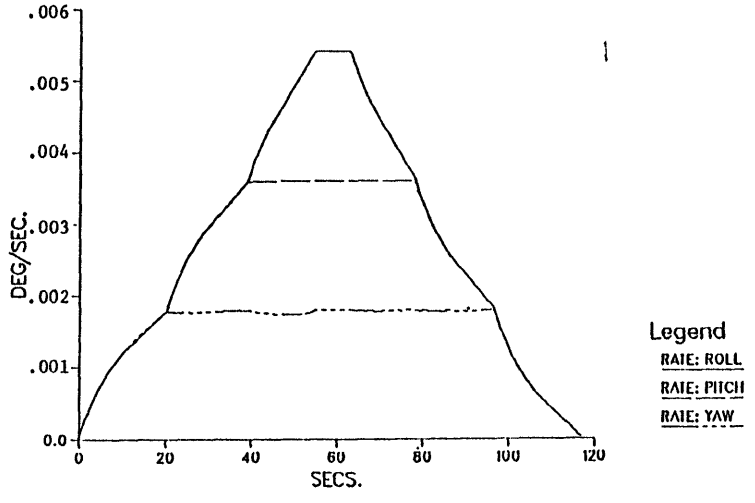

Outer Gimbal Stops Placed at 180°

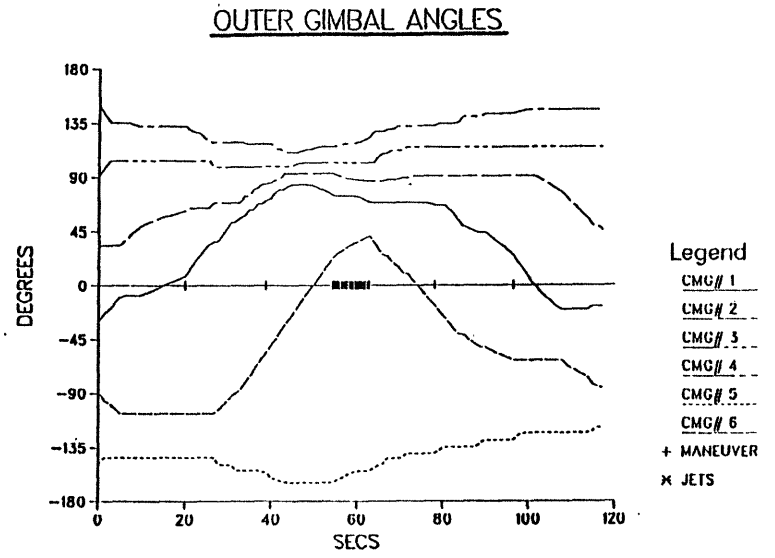

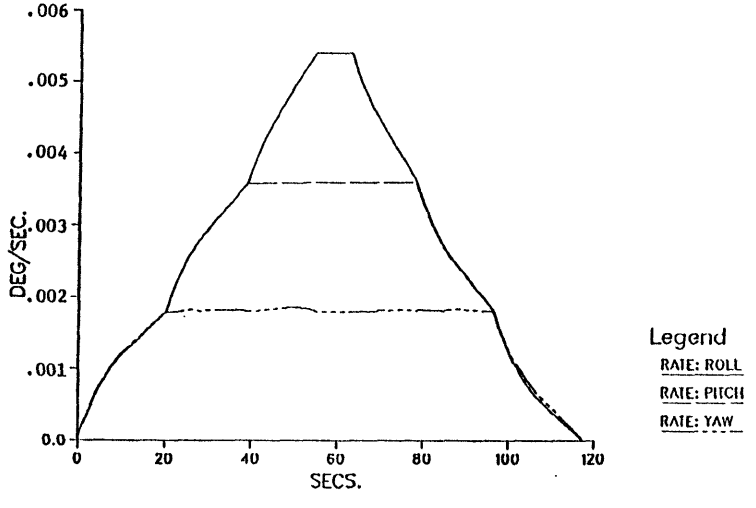

(Figure 2). A command sequence is input which builds, maintains, and removes peak rates of 0.0054, 0.0036, and 0.0018 deg/s along the vehicle roll, pitch, and yaw axes, respectively. Two tests are performed, the first assuming no stops on the outer CMG gimbals (as has been conventional), and the second imposing an outer gimbal stop at 180° (preventing rotation past this point). Outer gimbal angles and resulting vehicle rates are plotted in Figure 10 for both cases. In the nominal situation (left column), we see that two CMGs (#4 & #5) are indeed rotated through 180° in order to provide the requested rate profile (lower plot). The CMGs are used in a different fashion after the stops are imposed (right column). Although no outer gimbals cross 180° (where the stops are defined), a set of vehicle rates is produced (lower plot) which is identical to that obtained without gimbal stops.

Example #6: Demonstration of Null Motion

The term "null motion" refers to CMG gimbal redistribution that places the CMGs into a superior orientation without torquing the vehicle. Even though the objective function intrinsically accomplishes such redistribution while answering input requests, the ability to command the linear programming procedure to produce null rates and redistribute the gimbals without creating net torque may prove desirable (e.g., to restore controllability after the CMGs are initialized in a poor configuration). A null motion capability has been developed and integrated into simplex, as demonstrated in the following example.

This test assumes the Power Tower controlled by the standard quad orthogonally-mounted double-gimballed CMG array (Figure 3), and commands a series of requests which increase the vehicle rate along the pitch axis until momentum saturation is reached. The CMGs are initialized in a "sub-optimal" orientation of reduced controllability (with finite inner gimbal angles and rotor alignments), and null motion (as discussed earlier) now attempts to move the CMGs into a better orientation before the receipt of each input request.

Gimbal angles are shown in the left column of Figure 11. The upper plot shows inner gimbal angles; all are at a minimum by t = 30 s (as indicated). Excessive inner gimbal swings are otherwise seen to be avoided until a jet firing is required at t = 135 s.

Rotor alignment plots are given in the right column of Figure 11; the alignments are brought to a minimum by t = 30 s (as indicated). Jet assistance is required after the CMG rotors line up in saturation at the end of the run.

The saturation index is shown in the upper left of Figure 12; it exceeds unity at the points where jets were introduced, indicating a momentum saturation condition.

Quantities representing the degree of 3-axis CMG controllability have been plotted for this run in the lower left portion of Figure 12. The low value of CMG controllability (solid curve; termed "CMG gain") at the start of the run (due to the initial sub-optimal orientation) is restored to a maximum value by t = 20 s (as indicated). We see that the objective contribution which avoids rotor alignments has indeed maintained a high value of CMG controllability until saturation was reached and jet assistance was required.

The upper-right plot in Figure 12 shows the net CMG objective evaluation (corresponding to the "nonoptimality" of the CMG orientation). This is termed the "CMG cost", and is defined such that high cost values imply problematic CMG orientations (re. stops, inner gimbals, lineups, etc.); lower cost orientations are preferable. Asterisks are plotted over this curve where null motion was attempted. Its effect is plainly to decrease the CMG cost (thus achieve a superior CMG orientation). One sees that the relatively high cost of the initial sub-optimal orientation was reduced drastically by null motion which was performed at the start of the test; the minimum cost thus achieved is at t = 20 s (as indicated), which corresponds to the "best" physical orientation noted on the previous figures. Null motion is suspended when it can no longer achieve any further decrease in the system cost, or a significant command arrives from the operator or phase-space controller.

FIGURE 11: Demonstration of Null Motion

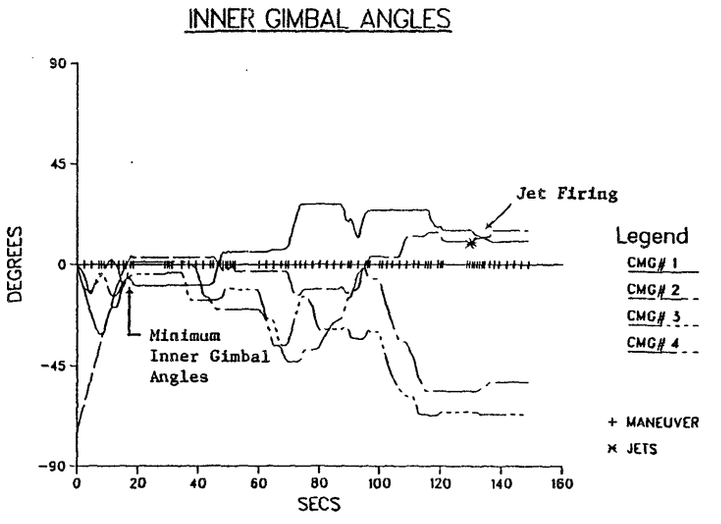

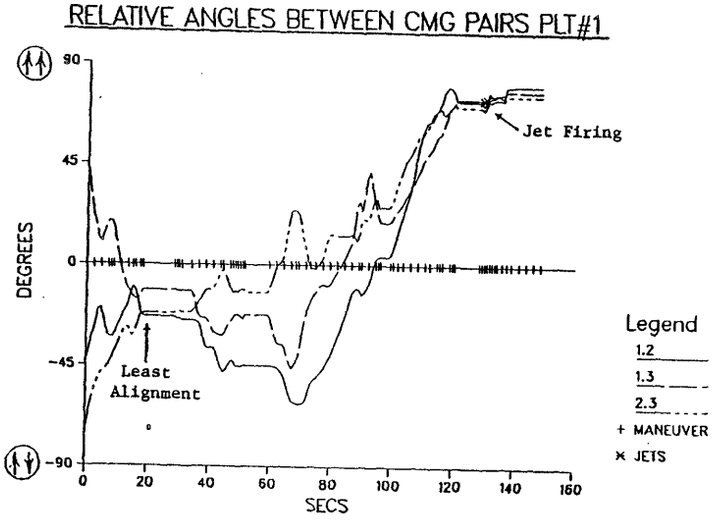

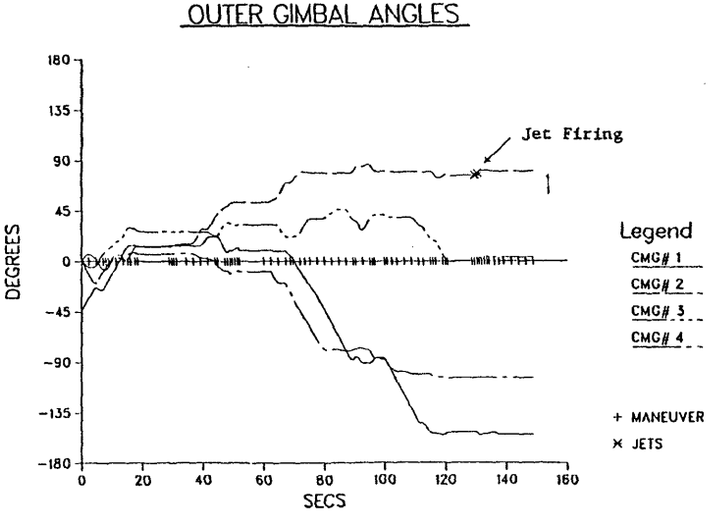

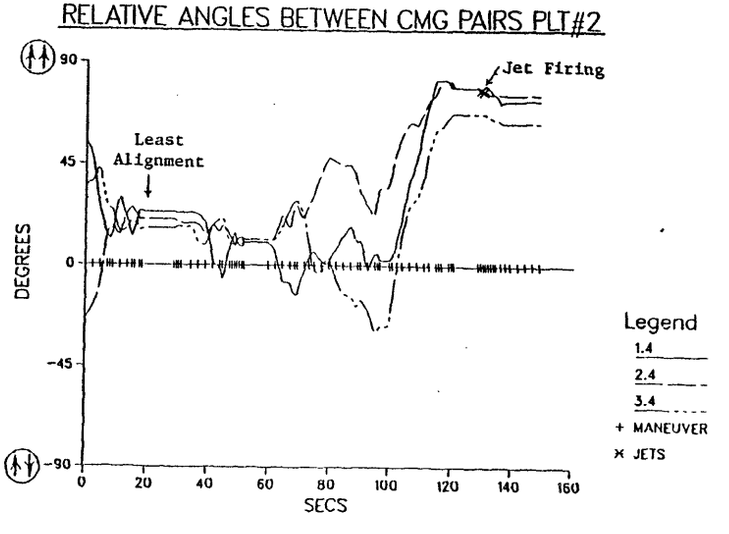

FIGURE 12: Demonstration of Null Motion (cont.)

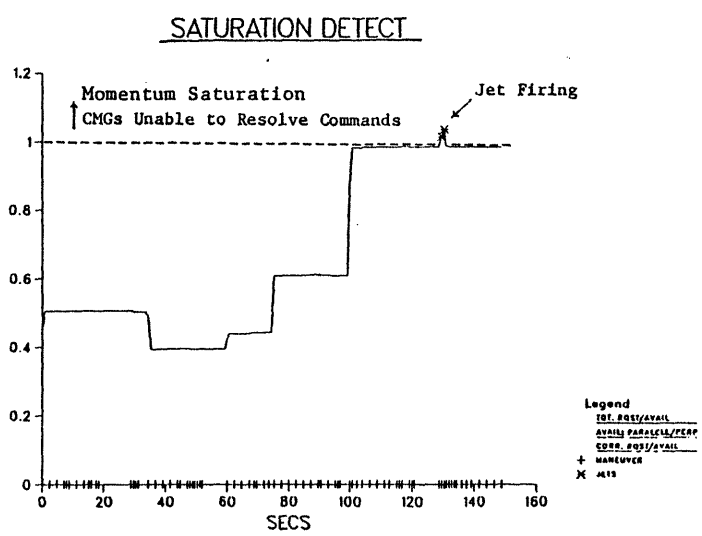

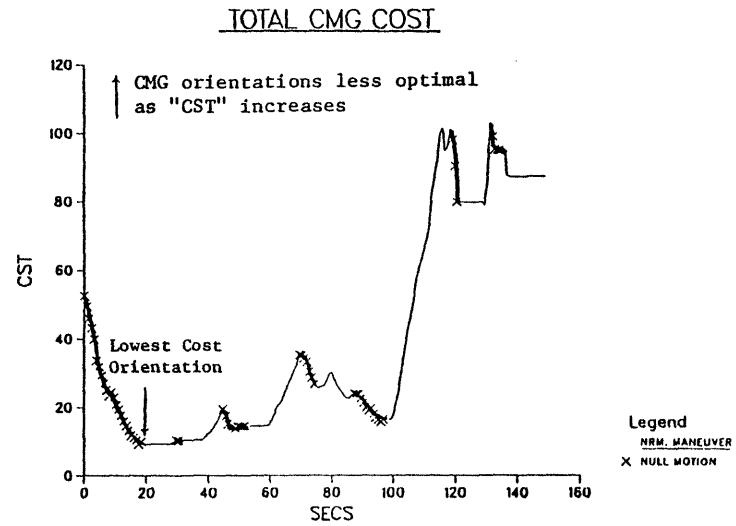

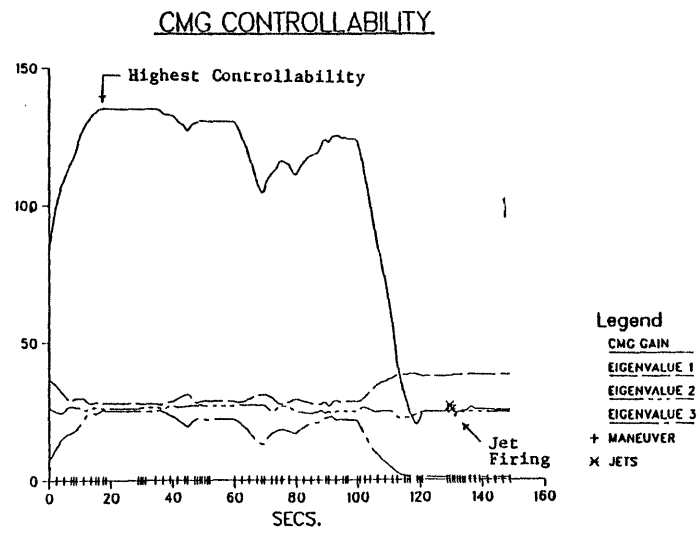

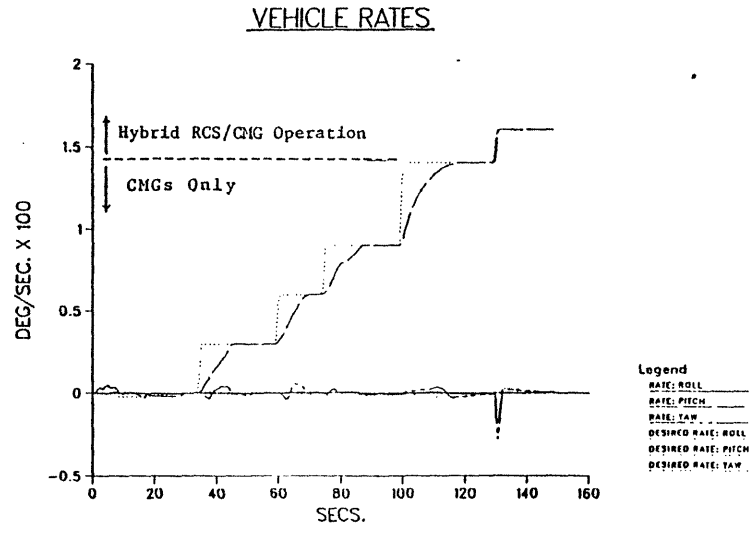

Vehicle rates are plotted in the lower right portion of Figure 12. The dotted curve represents the desired vehicle rate profile (which is commanded to increase in a series of discrete steps); the actual vehicle response is plotted in a heavier curve, and is seen to follow the input commands (note that the vehicle responds much more quickly at the last step, where jets were introduced). One sees that vehicle rates were indeed held constant while null motion was being performed. All rate-change commands were applied about the pitch axis; residual roll and yaw rates are seen to remain minimal (the vehicle attitude is commanded to hold at zero about these axes).

Example #7: Steering Systems of Single Gimballed CMGs

Because of their mechanical simplicity, torque amplification advantage, and lower weight, cost, and power requirements, single gimballed CMGs are preferred over double gimballed devices in many applications. Avoidance of singular configurations (where control is restricted to a single axis or plane) can be considerably more difficult, however, since singular states may not be directly related to particular geometrical properties (such as rotor alignments) in arbitrary single gimballed CMG configurations. A method of deriving objective factors from the gradient of the net CMG controllability index[3] has been developed to aid in steering single gimballed CMG systems to maximize 3-axis control authority and avoid singular orientations.

The next simulation example assumes the Power Tower to be driven by a pyramid-mounted array of five single gimballed CMGs (Figure 4). A series of rate increases (0.001 deg/s each) are commanded about the vehicle roll and yaw axes, eventually driving the CMG array into momentum saturation and forcing the introduction of jets. Yaw attitude is maintained at zero. Two tests are performed; one with no singularity avoidance in the objective, and another using maximum-controllability steering, as outlined above.

Resulting gimbal angles and saturation indices for both tests are shown in Figure 13. Each test exhibits similar behavior; i.e., gimbals are moved to achieve the desired momentum transfer while avoiding stops (CMG motion seems more responsive when gain steering is used), and CMGs step uniformly toward momentum saturation after each request is satisfied (jets are introduced to continue to meet commands after saturation).

The CMG controllability index (termed "CMG gain") and resulting vehicle rates are plotted in Figure 14. The right column shows results generated without including anti-singularity components in the CMG objective; significant drops in CMG gain (upper curve) occur at $t = 50$ s, and again when momentum saturation is reached at $t = 95$ s. These signify loss of 3-axis CMG control, and the effect of this control loss is evident in the vehicle rates (lower plot), where we see that the CMG system encounters difficulty achieving the commands.

The situation changes when the CMGs are steered to maximize CMG controllability; the large drop in gain becomes a gentle dip (the singular state is avoided), and 3-axis CMG control is maintained until momentum saturation is reached at $t = 95$ s. The identical set of vehicle rate commands are thus answered without difficulty throughout this test case.

Although the CMG controllability gradient aids in steering systems of single gimballed CMGs, it can not guarantee the avoidance of all singular orientations[3,4]. In order to attain more reliable performance, a more sensitive objective formulation must be employed which accounts for "global" CMG optimality and is able to detect singular states well before they are approached.

Example #8: Dynamic Definition of Peak CMG Gimbal Rates and Comparison With Other CMG Steering Laws

The maximum output torque of a CMG gimbal is proportional to the peak rate at which it can be rotated. In order to extend the lifetime of degrading CMG hardware, the ability to independently limit these

FIGURE 13: Saturate Single Gimballed CMGs along Roll/Yaw

Gain Steering Objective Used

GIMBAL ANGLES

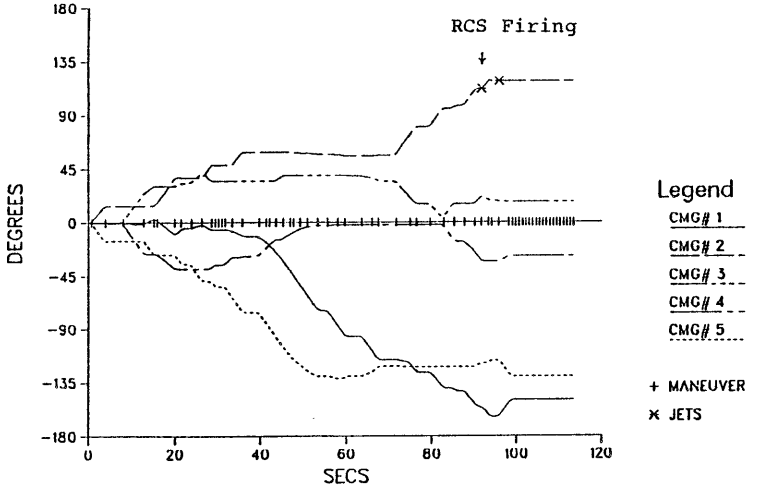

SATURATION DETECT

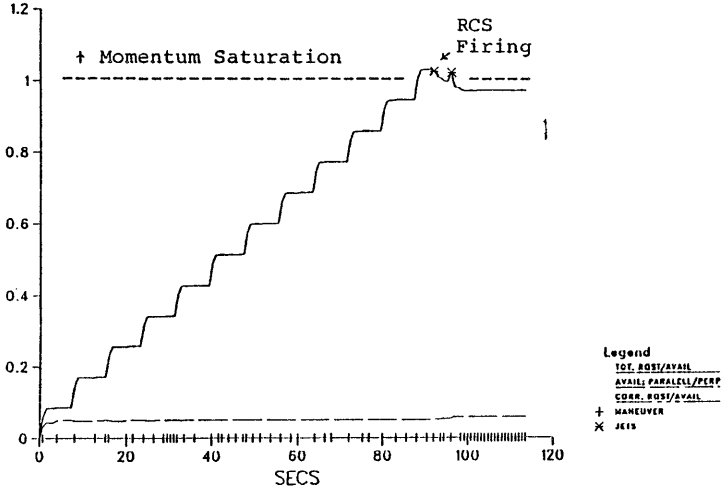

No Singularity Avoidance in Objective

GIMBAL ANGLES

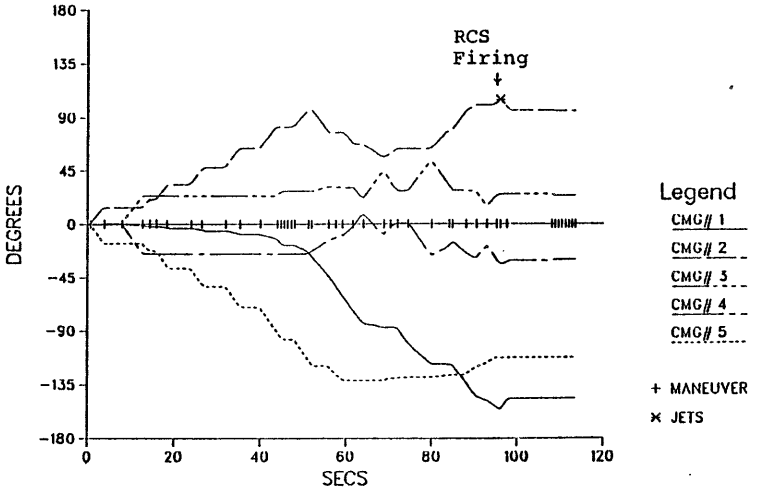

SATURATION DETECT

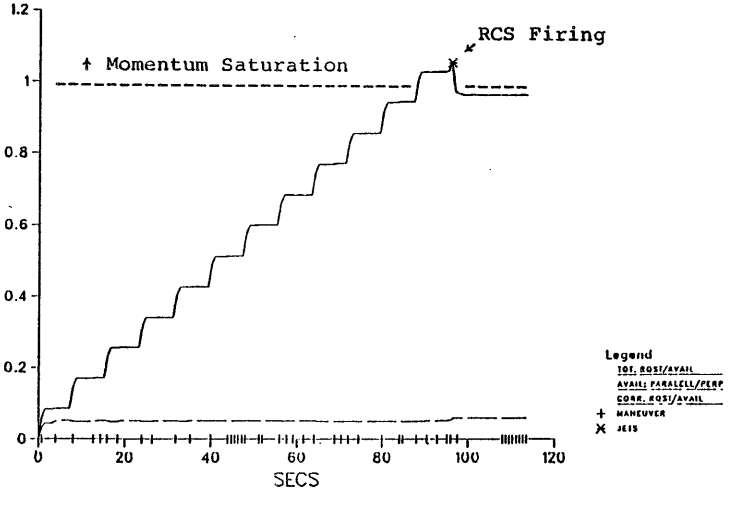

FIGURE 14: Saturate Single Gimballed CMGs along Roll/Yaw (cont.)

Gain Steering Objective Used

CMG CONTROLLABILITY

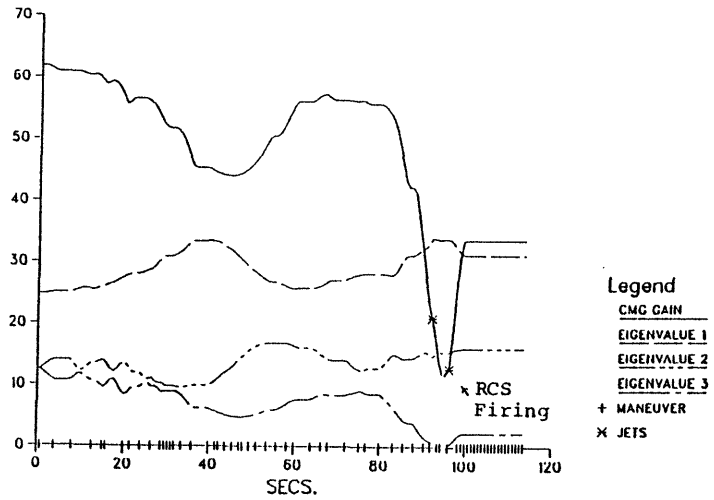

VEHICLE RATES

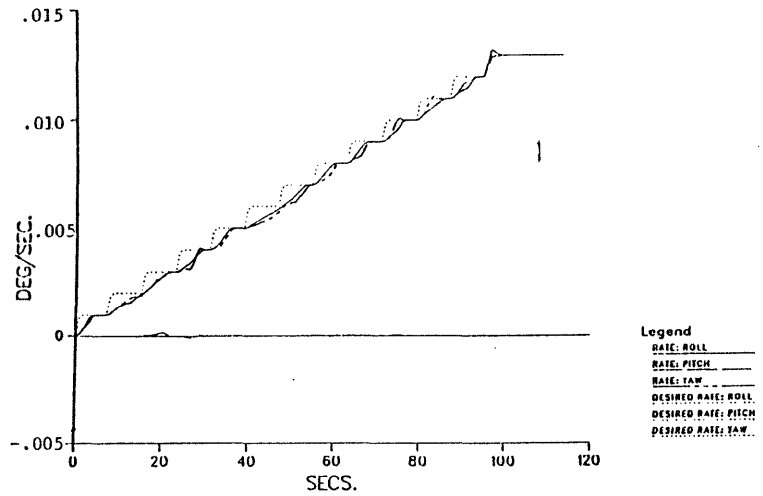

No Singularity Avoidance in Objective

CMG CONTROLLABILITY

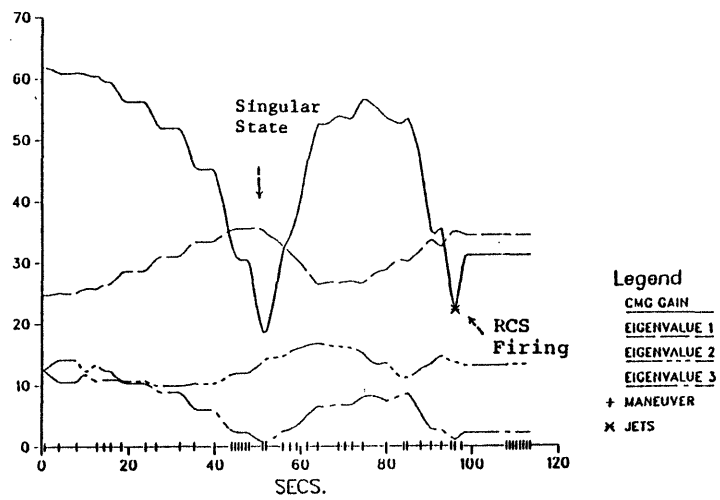

VEHICLE RATES

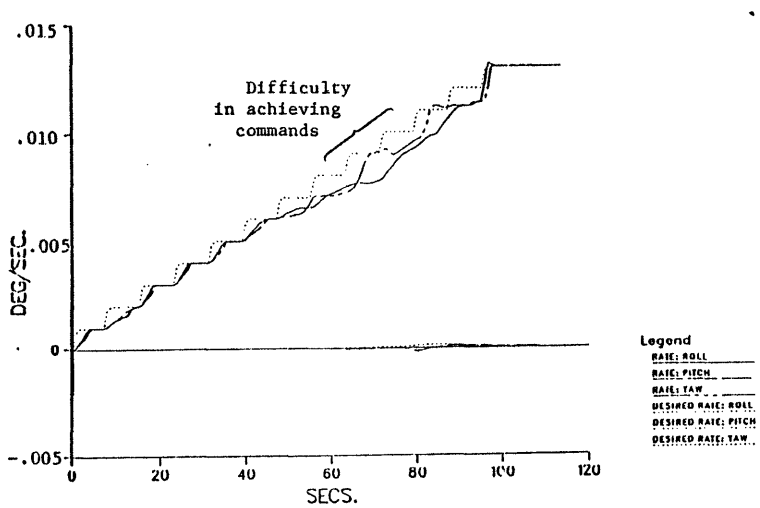

maximum rates may prove necessary. The overall performance of conventional (i.e., pseudoinverse) steering laws can suffer considerably when driving a group of CMGs constrained to operate at differing peak gimbal rates. Because of the separate upper bounds imposed on each gimbal when answering torque requests, however, the linear programming method is capable of obtaining maximum performance from a group of CMGs limited to arbitrary peak rates. This is illustrated in the following example.

A system of six parallel-mounted, double-gimballed CMGs (Figure 2) is assumed to control the Dual Keel configuration. Three of these CMGs can operate up to conventional peak rates of 0.09 rad/s (as has been previously assumed), while both gimbals of the remaining three units are constrained to rotate at less than 0.03 rad/s. The vehicle is commanded to increase its rate about the pitch and roll axes by an additional 0.00035 deg/s every two seconds throughout the duration of this test. Yaw rate is commanded to remain at zero. Two test runs are performed; one employs the steering law of Ref. 1 (which uses an approach "hardwired" to parallel mounting), and the other employs the linear programming selection described in this text. Both actuator management procedures are driven by the same control law, and both tests use the same input command sequence (as detailed above).

Gimbal angles are given in Figure 15. Results from the run using linear programming are shown in the left column. All inner gimbal angles (upper plot; inner gimbals provide the only means of controlling pitch under this mounting scheme) are seen to increase together until jets are required after approximately 33 s into the test. Outer gimbal angles are shown in the lower plot; these are seen to converge toward a common value (indicating approaching momentum saturation). In order to continue providing the torque required to satisfy input commands, jets are introduced shortly before the CMGs become saturated (the capacity of the CMG array to maintain torque along the saturation axis diminishes with the sine of the average inter-rotor half-angle as saturation is approached). The CMGs finish just short of saturation in this case; hybrid jet/CMG control is applied between t = 35 and 45 s,

after which the CMGs possess negligible authority about the commanded axis, causing a transition to mostly jet-based control.

The gimbal angles plotted in the right column of Figure 15 result from the test case that uses the steering law of Reference 1. The general behavior seems quite similar to the linear programming results. This steering law is directly optimized for parallel mounting (it will not work in its present form for any other configuration), and is subject to several constraints, one of which forces equal inner gimbal angles, as is evident from the upper-right plot in Figure 15. All outer gimbal angles are seen to converge to an identical value after $t = 51$ s, indicating momentum saturation (since this steering procedure alone does not possess the ability to exploit a different set of actuators for additional authority, CMGs are driven hard into saturation).

Vehicle rates from both steering laws are plotted in Figure 16. Desired rates are shown as the increasing dotted staircase; actual vehicle rates are denoted by heavier curves. The linear programming results are plotted at left, where we see that the CMGs are able to supply the torque needed to meet the input requests until momentum saturation is approached, at which point jets are gradually introduced to continue satisfying commands. The higher control authority of the jets is evident in the quicker vehicle response at the end of the run.

Vehicle rates arising from the steering law of Reference 1 are plotted on the right side of Figure 16. It is immediately evident that the CMGs are now unable to supply sufficient torque to meet the input commands (even though identical CMG hardware definitions are used). This arises from the inability to specify independent rate limits for each CMG gimbal; when this steering law exceeds at least one maximum gimbal rate, all gimbal rates must be scaled down proportionally such that every gimbal is operating within limits. In a mixed configuration such as assumed in this example (where half of the gimbals are constrained to run below reduced maximum rates), the response generated from a large input torque request will often specify at least one of the degraded gimbals at a rate above its limit, causing all gimbal

FIGURE 15: Dynamic Definition of Peak CMG Gimbal Rates

Hybrid Controller

INNER GIMBAL ANGLES

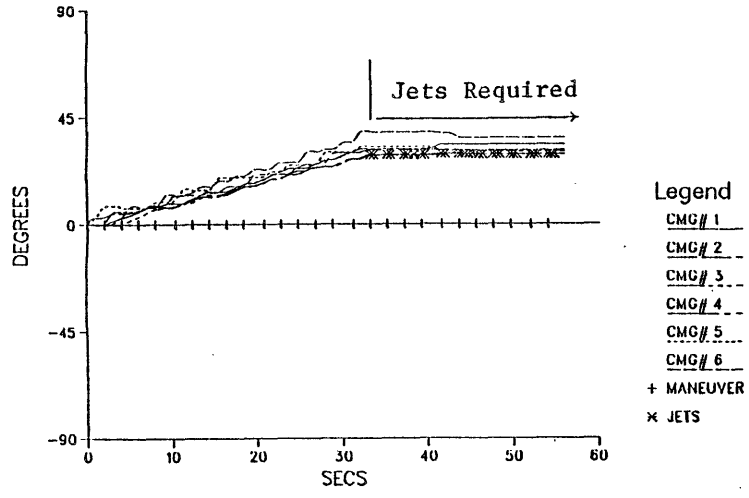

OUTER GIMBAL ANGLES

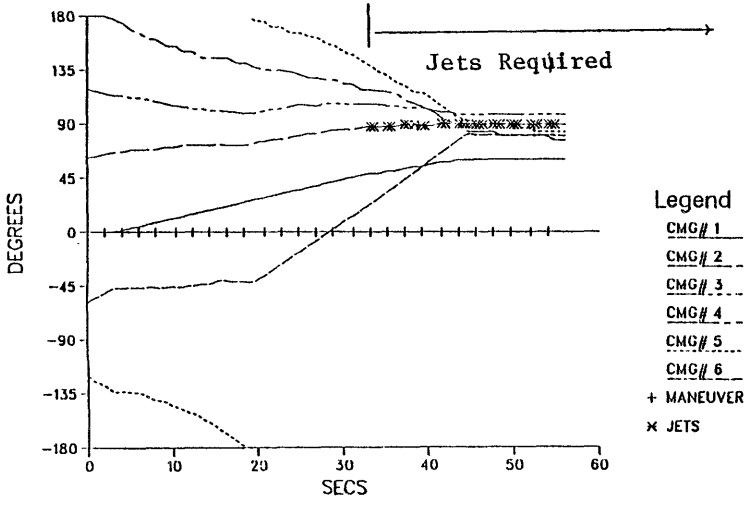

Kennel's Law

INNER GIMBAL ANGLES

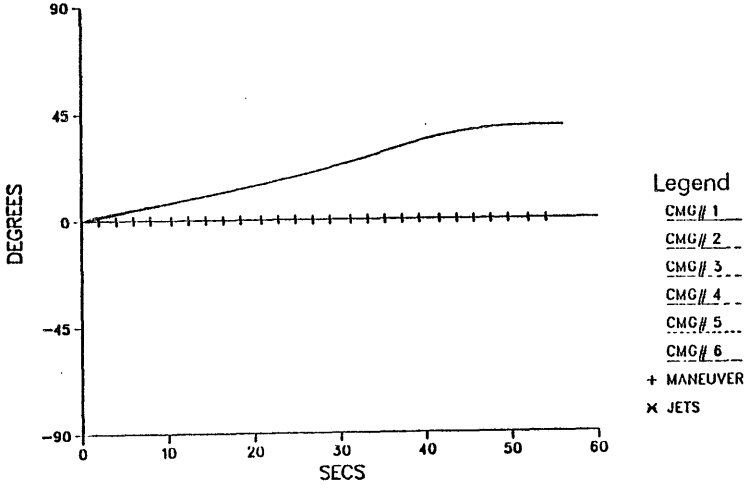

OUTER GIMBAL ANGLES

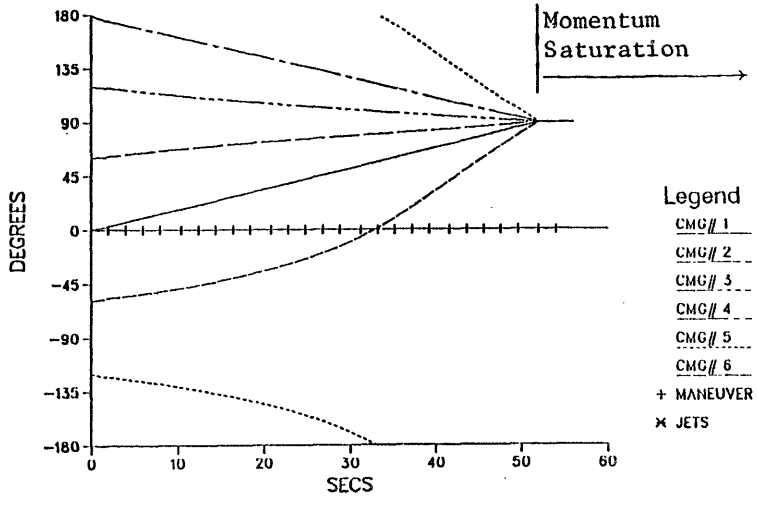

FIGURE 16: Dynamic Definition of Peak CMG Gimbal Rates (cont.)

Hybrid Controller

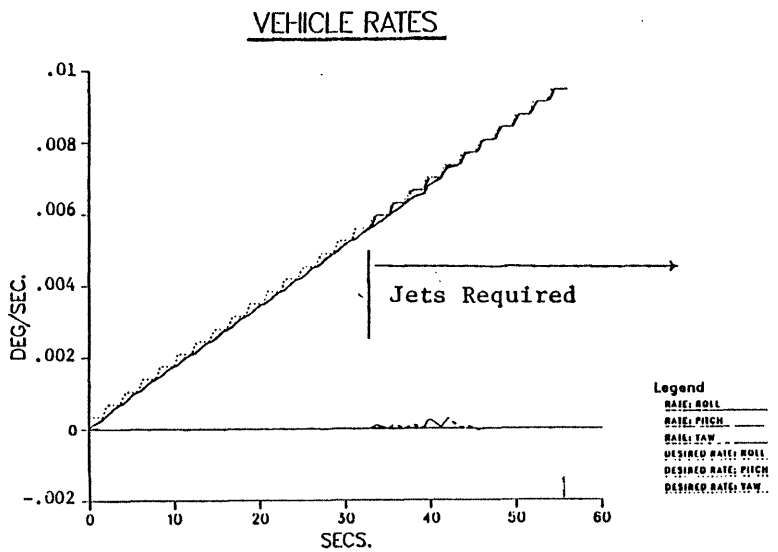

Kennel's Law

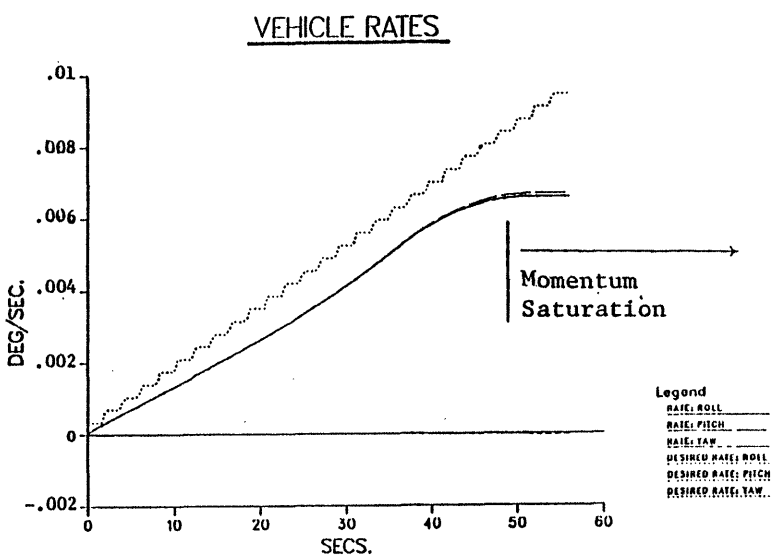

rates to be scaled down accordingly and resulting in the net CMG system being driven below capacity.

Since the steering law of Reference 1 has no provision to select any other actuators, the available output torque eventually decreases as momentum saturation is approached, and the system is unable to realize any rates greater than 0.0065 deg/s (simultaneously about roll and pitch). The hybrid selection gradually introduced jets to compensate for the lower CMG torque capacity near saturation (if jets were inhibited, however, the linear program would also align the CMG rotors in hard saturation, causing the achieved vehicle rate to likewise plateau).

The steering law of Reference 1 calculates null CMG redistribution rates independently from torque-producing gimbal motion, and sums both to form its final solution. If the redistribution rates become significantly large, they can prematurely limit the magnitude of available torque-producing gimbal rates, thereby causing the CMG system to be run below capacity. The linear programming selection accomplishes CMG redistribution by optimizing the assignment of gimbal rates through an objective function; all solutions provided by the simplex procedure meet the input request, and no additional "redistribution" rates are added afterward.

The steering law of Ref. 1 exploits many properties of the parallel-mounted double-gimballed CMG configuration in order to achieve its level of performance. Because of this, it lacks much of the flexibility of the linear programming approach; i.e., abilities to assume any mounting orientation, effectively impose different maxima on individual CMG gimbal rates, fail individual CMG gimbals, impose arbitrary gimbal stops, and blend other actuators through hybrid selections.

Example #9: Coordinated Control of Vehicle Translation and Rotation

Translational maneuvers will be executed during normal operation of the space station, both periodically (i.e., orbital re-boost) and

upon demand (i.e., evasive action). Translational control authority is derived from the onboard system of reaction control jets. Because jet placements are generally offset from the vehicle center of mass, each jet also generates a torque while firing. If translational jet selections are performed without maintaining rotational control, the vehicle attitude will drift as jets are firing, causing the direction of translational thrust to shift correspondingly. The linear programming jet selection can be expanded to fire up to six jets at a time (even more could be included in a solution if upper bounds are used), thereby enabling simultaneous translational and rotational control. The corresponding autopilot assumes, however, that jets instantaneously impart their impulse to the vehicle. Although this may be a reasonable assumption for maneuvers employing short jet pulses, the necessary firing durations will be quite long when a larger translational rate is desired (as is certainly true during orbital re-boost). If the applied jets are not aligned in a perfectly balanced configuration (i.e., at equal moment arms from the vehicle center of mass), the firing times will differ for various jets in the solution in order to balance their mismatched rotational impulses. This generates a finite torque throughout the burn that changes after each jet is shut down. Although the vehicle rotational rates will reach the desired values at the close of the maneuver (as per the 6-dimensional input request), the dynamic torque imbalance can cause the vehicle to exhibit considerable undesired rotation while jets are active, leading to the accumulation of significant attitude errors. In order to maintain the desired vehicle attitude during translational maneuvers (and thus control the translational thrust vector), sets of jets are generally "cycled" on and off, compensating on average for this torque imbalance. Unless jets are cycled very rapidly, this strategy will generally result in a "swaying" vehicle motion during translation, where a change in the jet firing is forced such that the direction of vehicle rotation is reversed whenever significant attitude errors have accumulated.

The linear programming selection has been applied to investigate the possibility of using CMGs together with jets in order to stabilize vehicle rotation during translational maneuvers. The simplest method of coordinating jet and CMG activity in this case is to perform a 6-dimensional hybrid selection; CMGs will be specified to aid in rotational control, while translational authority will be provided exclusively via jets. This is an effective strategy for short translational pulses; the objective function will encourage CMG motion that tends toward desaturation, and the RCS fuel demand may be reduced. To build up significant translational rates on a massive spacecraft such as the space station, however, long-duration firings will be required, hence such hybrid selections will be of limited value due to the large differences in control authority between CMGs and jets.

Another strategy has been pursued to combine jet and CMG activity during translational maneuvers. Provided that the CMGs can yield sufficient output torques and have enough momentum capacity to maintain this torque during significantly long jet firings, the CMGs may be commanded independently to null the jet imbalance during translational maneuvers and maintain steady vehicle attitude.

A set of simulations has been performed to illustrate this means of coordinating rotational and translational control. The Dual Keel configuration (with 10 lb thrusters) is used with an array of six parallel-mounted double-gimballed CMGs (Figure 2). The input command sequence consists of a request to achieve and remove a .05 ft/s translational rate along the vehicle x-axis. The vehicle attitude and rotational rates are actively compensated by a proportional/integral feedback controller which operates after the translational jet firings are completed. Vehicle rates are nulled to within 10^{-4} deg/s and attitudes to within $3x10^{-4}$ deg. before another firing is attempted. Two test runs are performed; one inhibiting all CMG activity during the translational firings (CMGs are used to restore vehicle attitude afterwards), and another using CMGs to dynamically null the jet imbalance torques.

Gimbal angles are shown in Figure 17. The example using uncompensated jet firings is shown in the left column, while results employing dynamic CMG torque compensation are shown at right. In the latter case, most CMG motion is seen to occur during the jet firings, while in the former example, all CMG activity happens after jets have ceased operation. Although the jet firings are on the order of 50 s each, the CMGs do not approach saturation in either example.

Vehicle rates and attitudes are shown in Figure 18. The uncompensated case is shown in the left column. Although vehicle rates are seen to return to zero at the conclusion of the jet firings (as indicated), the vehicle must be rotated additionally to null accumulated attitude errors (of order 0.25 deg.). Vehicle rates and attitude errors occurring under dynamic torque compensation are plotted to the same vertical scale in the right column. Because the CMGs were able to dynamically null nearly all torques during jet firings, residual vehicle rates and resulting attitude errors are seen to remain negligible. As mentioned earlier, the controller commands the second jet firing as soon as vehicle attitudes and rates are returned to within allotted deadband limits; since the rotational disturbance is much smaller during the actively compensated test, any residual errors are removed much more promptly, and the simulation is completed in less than half of the time required without compensation (note the difference in horizontal axis scaling).

Translational rate and relative position changes are plotted in Figure 19. Jet firings established and removed the .05 ft/s translational velocity without difficulty. The vehicle coasted at constant velocity while CMGs trimmed residual attitude errors. The shorter duration of the compensated test (as explained above) resulted in a 5-ft vehicle displacement, vs 10 ft. for the uncompensated example (due to the longer coast interval).

One could easily extend such compensated jet firings by stacking one immediately after another. Attitude errors will remain minute (any residual error can be removed by commanding a small rate offset in the succeeding firing cycle), and the CMGs always finish in a zero-momentum

FIGURE 17: Coordinated Control of Translation and Rotation

No CMG Motion During Jet Firings

INNER GIMBAL ANGLES

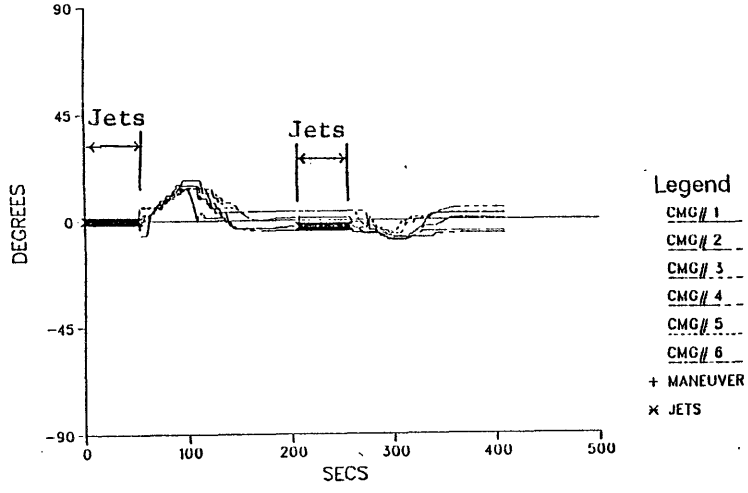

OUTER GIMBAL ANGLES

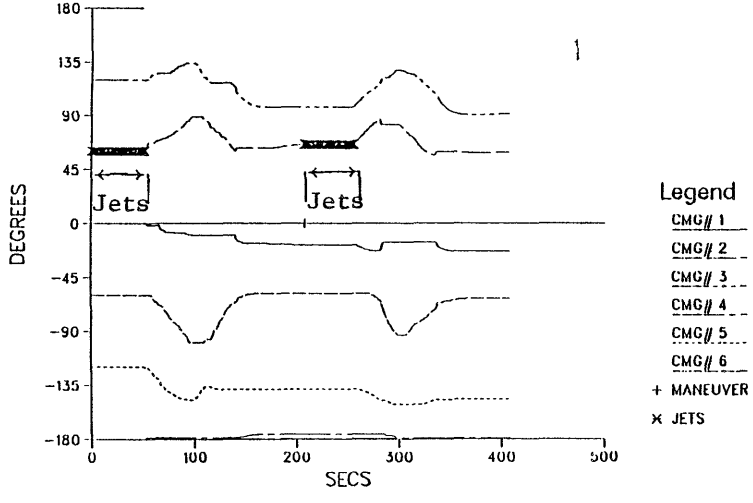

Jet Firings Actively Compensated

INNER GIMBAL ANGLES

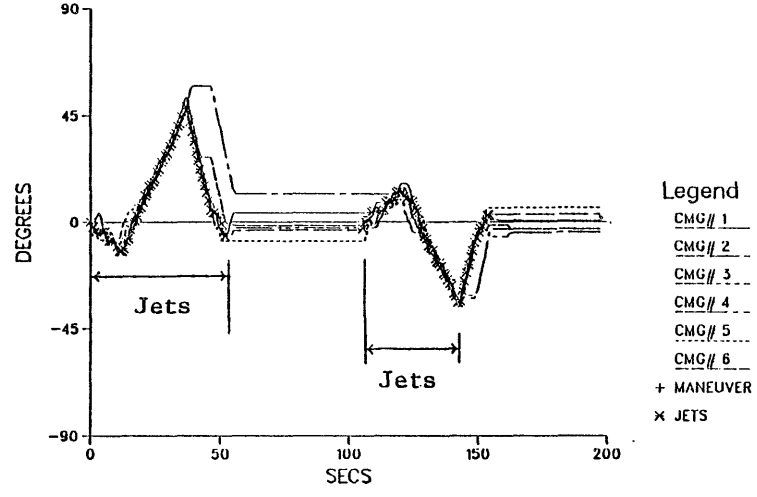

OUTER GIMBAL ANGLES

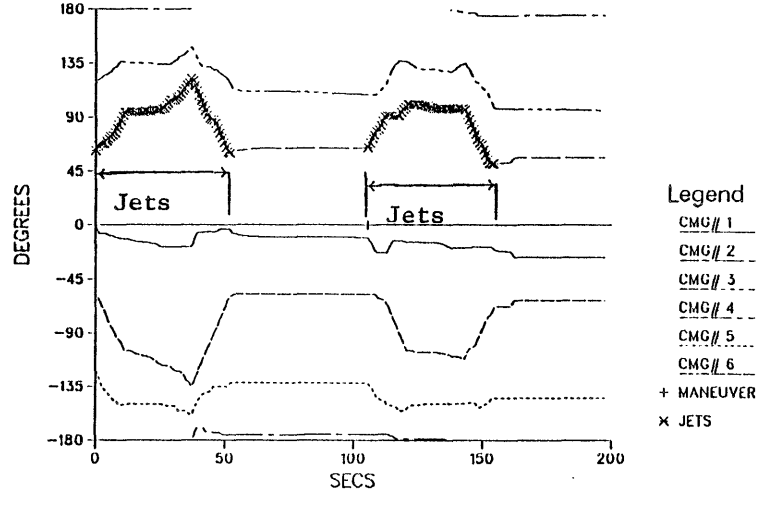

FIGURE 18: Coordinated Control of Translation and Rotation (cont.)

No CMG Motion During Jet Firings

VEHICLE RATES

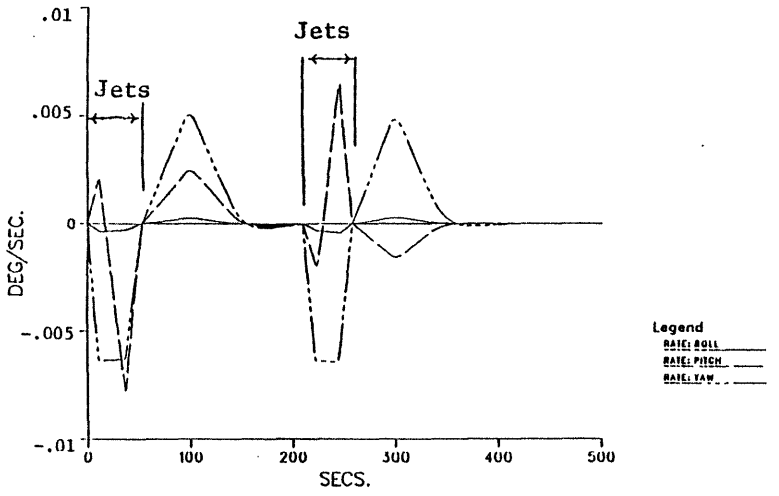

VEHICLE ATTITUDE

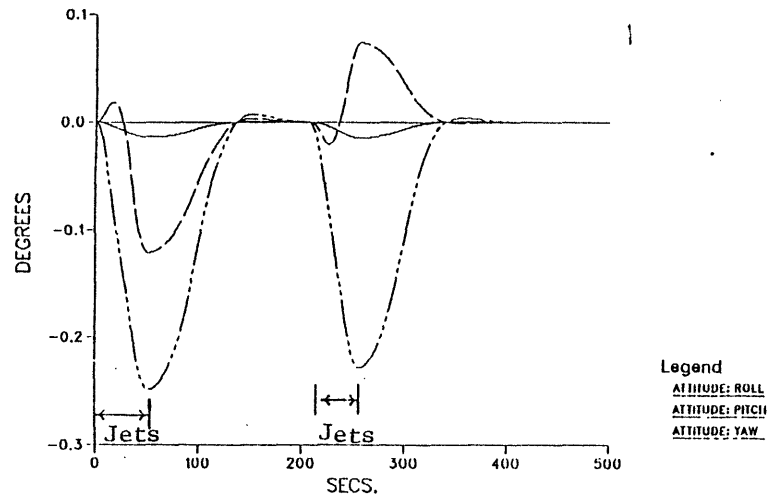

Jet Firings Actively Compensated

VEHICLE RATES

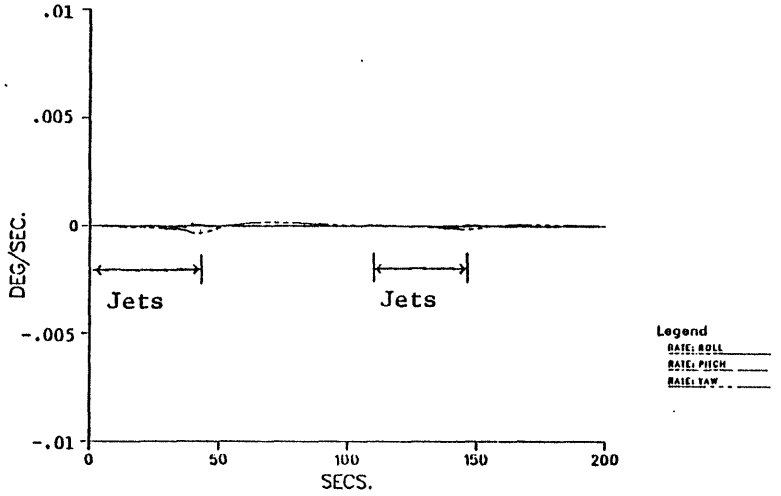

VEHICLE ATTITUDE

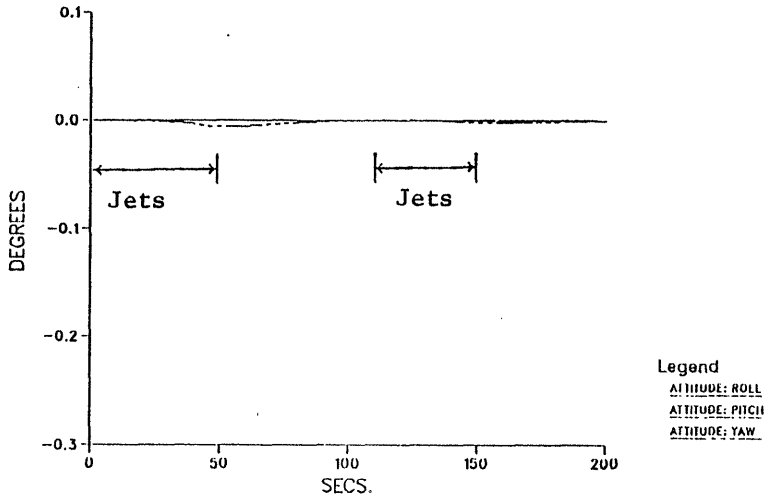

FIGURE 19: Coordinated Control of Translation and Rotation (cont.)

No CMG Motion During Jet Firings

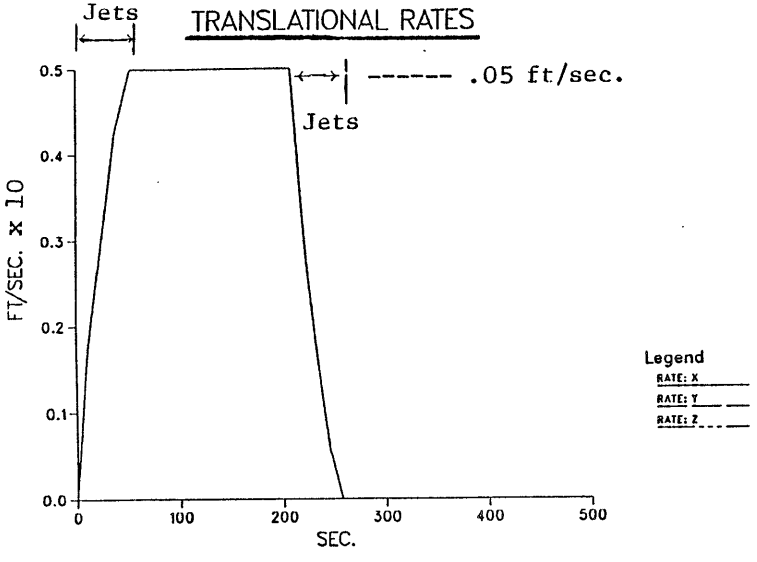

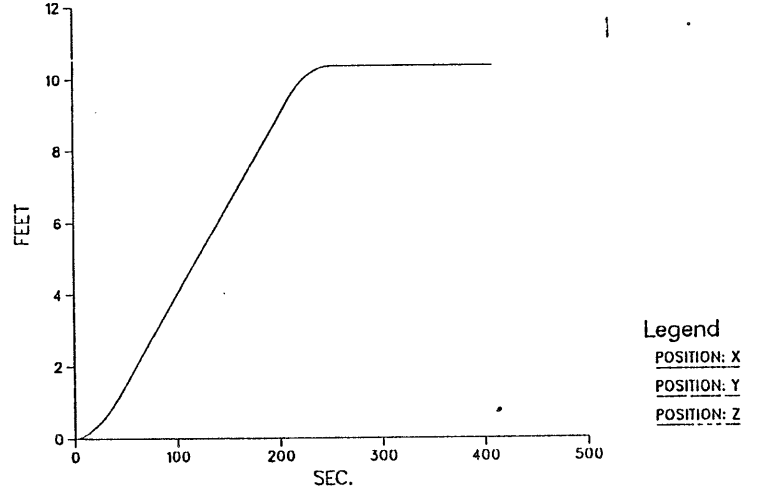

Jet Firings Actively Compensated

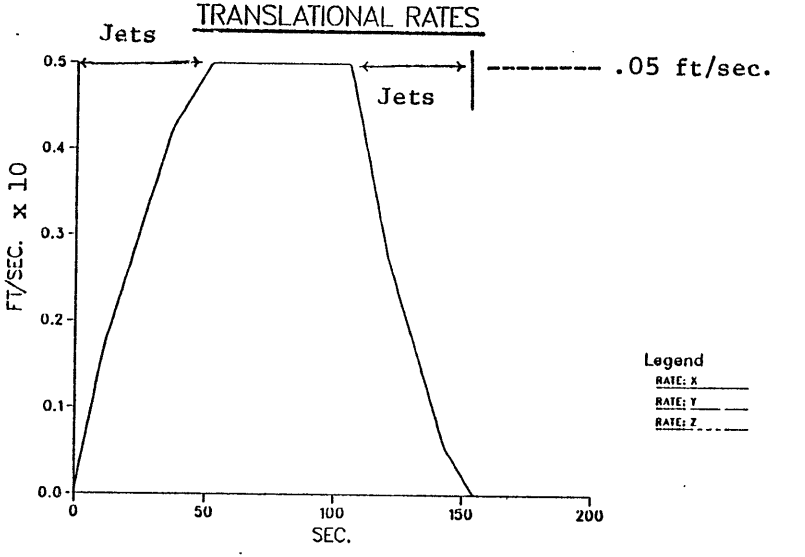

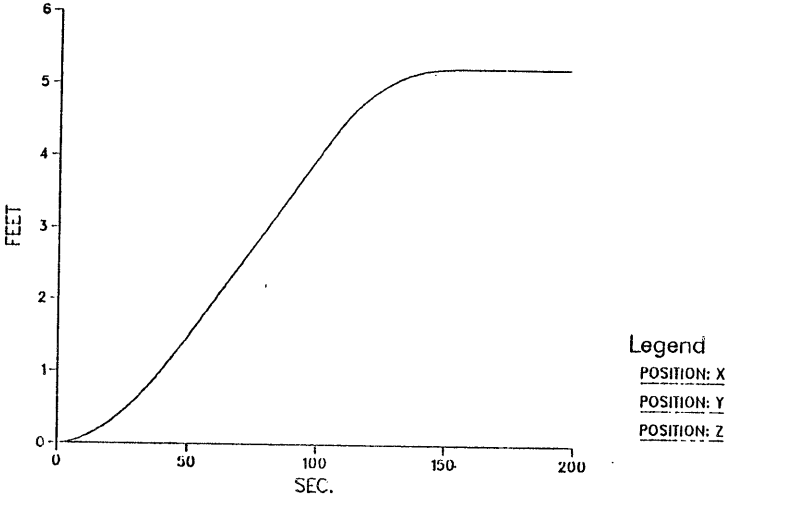

state (provided that they have not torque-saturated during the maneuver). Since small 10-lb thrusters were assumed in this example, this strategy, as demonstrated, might be directly applicable to local maneuvering of the space station (i.e., evasion, rendezvous). Re-boost operation, however, may be accomplished under significantly higher thrust (i.e., several parallel jets firing at each location), which would create significantly larger torques. If CMGs are to be employed for active compensation in this case, either the jets must be placed more symmetrically about the vehicle center-of-mass (although a well-balanced jet configuration will prove impossible to maintain in a dynamic vehicle such as space station), or more/larger CMGs must be employed to yield sufficient torque output and momentum capacity. It must be noted that these simulations have been conducted on a rigid-body model; for actual implementation, flexible modes must be taken into account and the average jet cycling times must be placed away from structural resonances.

This example has demonstrated how the linear programming approach has been applied to command jets and CMGs for coordination of translational and rotational control. The method of active torque compensation could also be used to improve the accuracy of purely rotational multijet firings. Given sufficient CMG authority, moderate changes in torque due to jets turning off at staggered intervals could be dynamically compensated by the CMGs such that the vehicle is subject to a constant torque through the duration of the maneuver.

c) On-Orbit Performance

The preceding examples demonstrated the performance and features of the linear programming selection/steering process by commanding a rigid-body space station model to execute specific inertial maneuver sequences. The next series of tests model a more realistic orbital environment in order to examine the behavior of the selection/steering approach as it would be implemented onboard an actual spacecraft.

A block diagram of the basic control law used to hold LVLH attitude appears in Figure 20. An estimate of net on-orbit

environmental torque is derived from calculations[13] of aerodynamic drag and gravity gradient components, which depend upon vehicle attitude and orbital position. These are summed with the inertial torques due to vehicle Euler coupling and LVLH CMG precession to form a net environmental disturbance. This disturbance torque is combined with feedback from the vehicle LVLH attitude error and rate (scaled by the gains K_1 and K_2), and submitted to the linear programming selection/steering package as a torque request (if jets are required, the hybrid selection will automatically solve for a vehicle rate-change which assumes that the input torque request is active over a pre-specified time interval).

The vehicle controller and environment are updated at one-second intervals in these examples. All tests use a 6-CMG double-gimballed configuration (mounted as specified; hardware parameters were defined earlier) to control the rigid-body Dual Keel Space Station model[10]. All jets are sized at 10 lb. thrust. These tests assume a circular orbit at 400 km altitude, and all examples are 6000 s in duration (i.e., 1.08 orbits). In order to accumulate sufficient torque over a single orbit such that CMGs are used significantly, the vehicle fabrication coordinates are assumed (which, adding a full set of payloads, are offset from the principal axes by approximately -7° in roll, -6° in pitch, and -0.5° in yaw). The vehicle is commanded to be additionally rotated about pitch such that averaged gravity gradient and aerodynamic torques are balanced over an orbital period.

The effects of environmental torques are evident in Figure 21, which shows the LVLH vehicle rates and attitude errors developing across an orbit for a freely drifting vehicle (note that these plots are in orbital coordinates, and do not show orbital rates or initial attitude offsets). The largest rates develop about the vehicle roll and yaw axes, and arise from the action of unbalanced aerodynamic and gravity gradient torques (respectively) together with Euler coupling. Because of the gravity-gradient/aerodynamic torque balance in pitch (plus lack of orbital Euler coupling), disturbances remain comparatively low about this axis. In summary, vehicle rates are seen

FIGURE 20: On-Orbit Controller

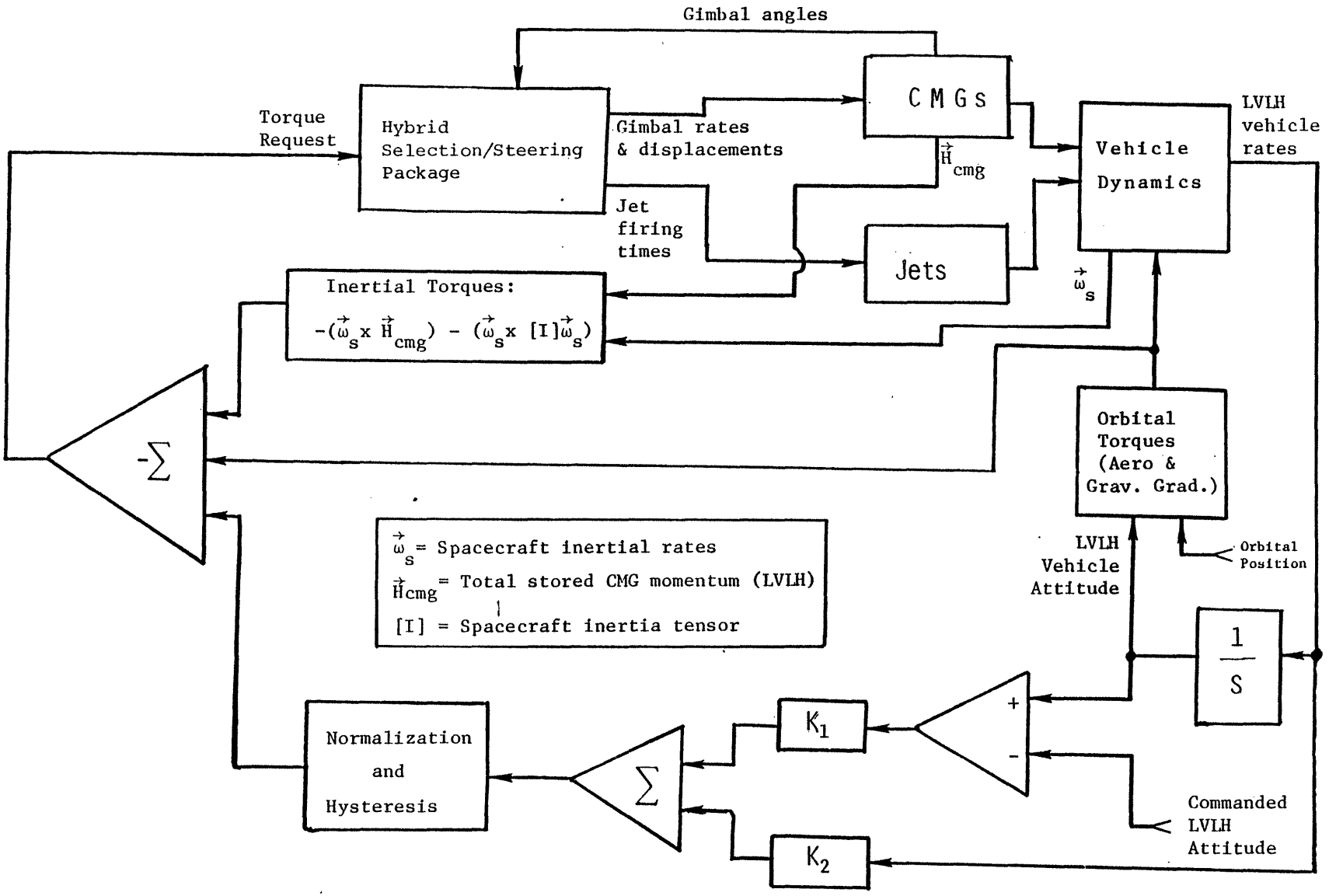

FIGURE 21: Uncontrolled Vehicle Response to On-Orbit Environment

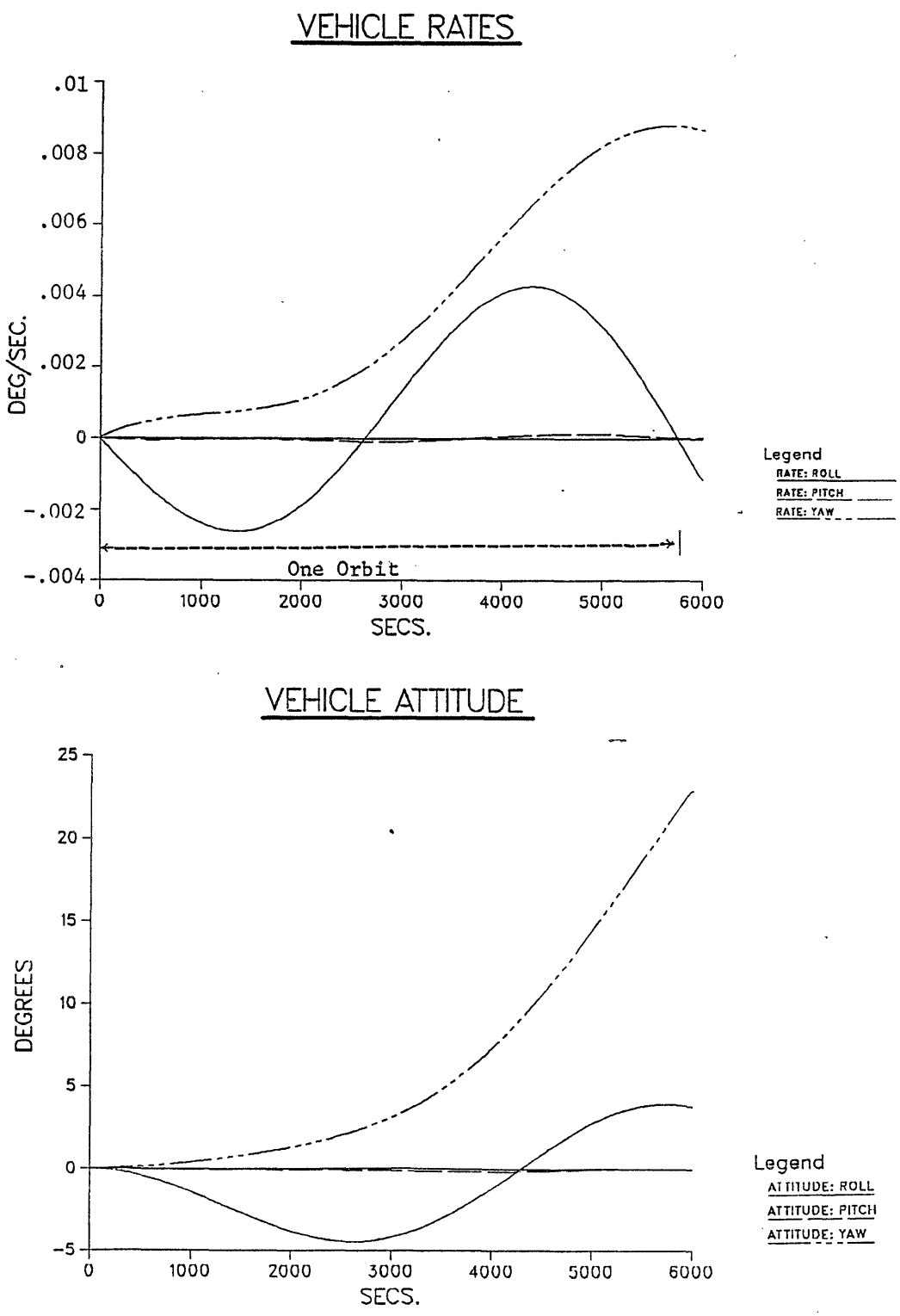

to approach 0.009 deg/s, and attitude errors surpass 20 deg. at the close of an uncontrolled orbit (assuming initial conditions as described above). This simulation serves as a baseline against which the following examples (which stabilize vehicle attitude via the controller sketched in Figure 20) can be compared.

Example #10: Nominal On-Orbit Operation with Parallel-Mounted CMGs

This example uses a standard parallel-mounted CMG configuration (Figure 2) in order to stabilize vehicle attitude throughout the orbit. Gimbal angle profiles are shown in the left column of Figure 22. Since the objective function encourages inner gimbal angles to be kept minimal (and inner gimbals provide exclusive pitch authority for this mounting orientation, thus require only minor adjustment over a torque-balanced orbit), they are seen to remain small. As was noted in Figure 21, most disturbance occurs about roll and yaw axes; thus we see considerable outer gimbal activity in order to null these torques. Outer gimbal angles are seen to begin converging (indicating approach of momentum saturation) at approx. t = 2500 s, yet the system is still sufficiently far from saturation to retain control without difficulty.

Vehicle rates and attitudes are plotted in the right column of Figure 22. Disturbances are insignificant; LVLH vehicle rates remain well below 0.0001 deg/s (thus are unable to be resolved in these plots), yielding attitude errors well under one arc second (in the actual vehicle, limited sensor resolution and environmental "noise" due to astronaut activity and mechanical operation would preclude any such accuracy; this idealized orbital environment is assumed here for test purposes only). The effects of active control are evident when these results are compared with Figure 21; the CMGs are driven to effectively null orbital torques and maintain vehicle attitude.

Example #11: Nominal On-Orbit Operation with Ortho-Mounted CMGs

The linear programming approach to CMG steering allows any CMG mounting protocol to be defined (this capacity is not supported by most

FIGURE 22: Nominal On–Orbit Operation with Parallel–Mounted CMGs

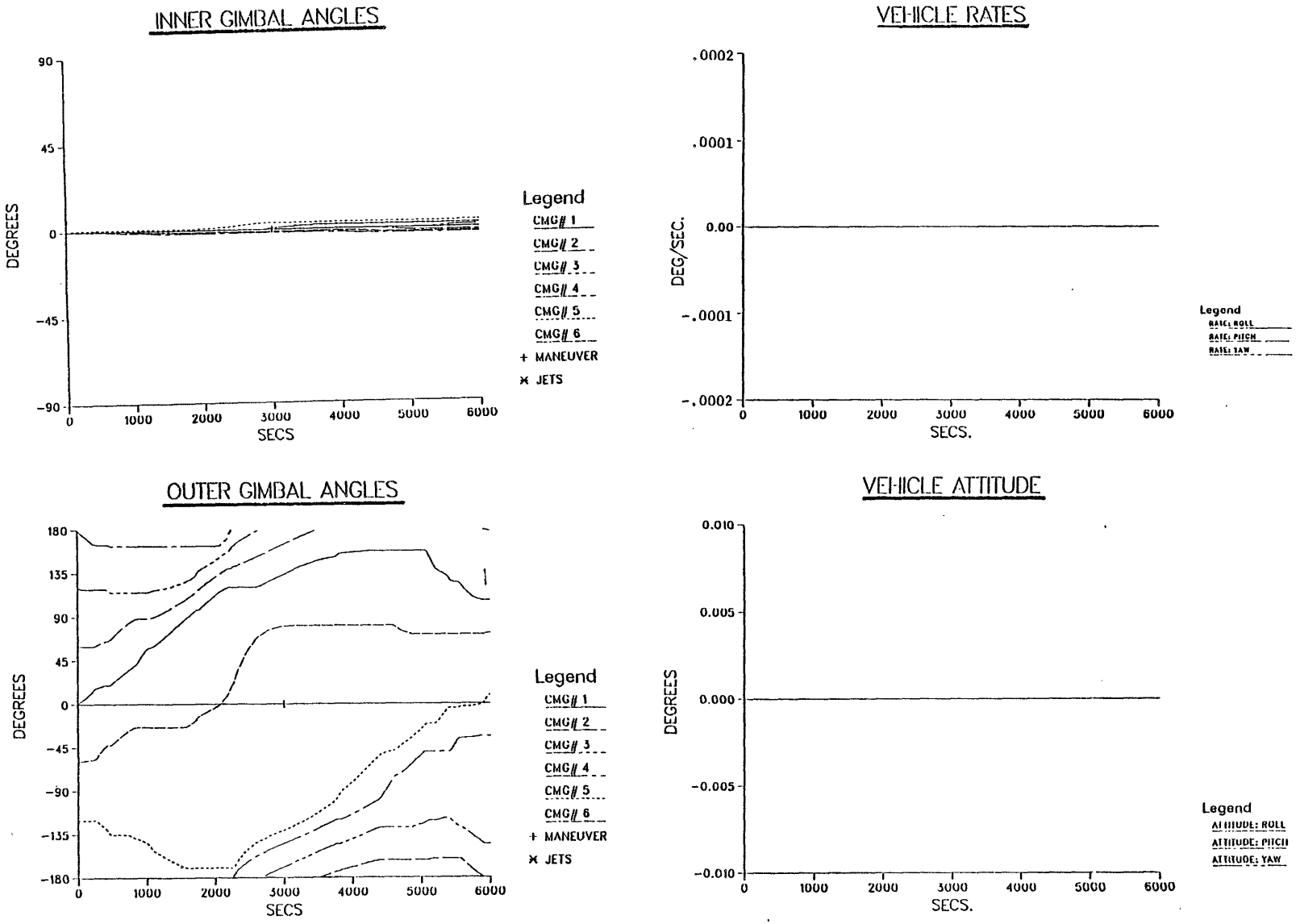

FIGURE 23: Nominal On–Orbit Operation with Ortho–Mounted CMGs

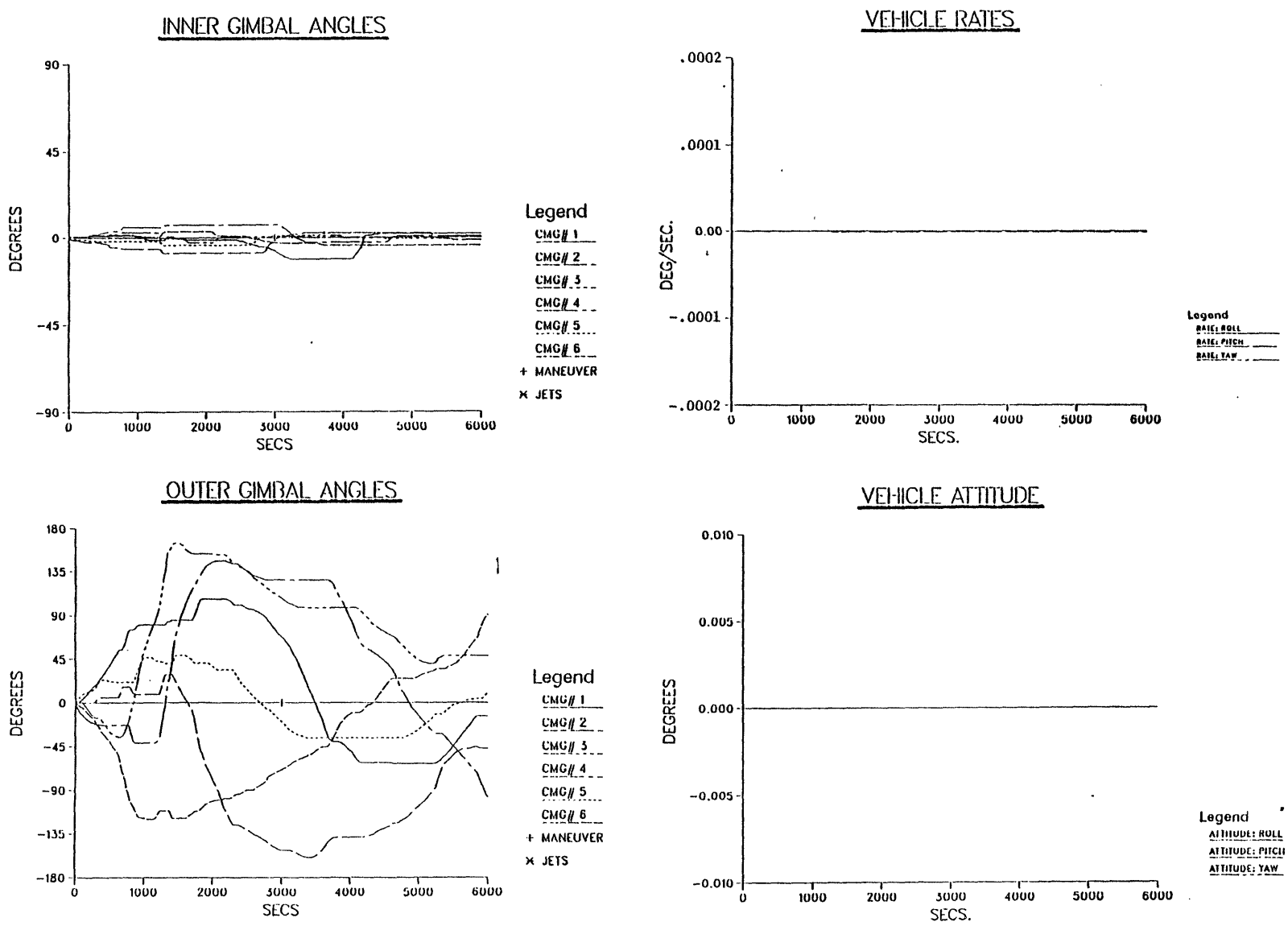

steering laws, e.g., Reference 1). Physical constraints onboard spacecraft may favor alternate CMG mounting schemes; these may be specified arbitrarily under this selection/steering principle.

The following example illustrates this point by performing on-orbit attitude control of the Dual Keel with an orthogonally-mounted 6-CMG configuration (Figure 3). Gimbal angles are shown in Figure 23 (left column). Inner gimbal angles are encouraged to remain minimal by the objective function, and this is what is indeed seen in the upper-left plot. Extensive outer gimbal activity is performed to compensate the environmental torques. Attitude and rate perturbations (right column) remain insignificant throughout the orbit, as established in the previous example.

Example #12: Hybrid On-Orbit Operation After Two CMG Failures

Another unique feature of the linear programming approach is its ability to coordinate the operation of different types of actuators under a hybrid selection. At the start of this example, the Dual Keel is controlled by six parallel-mounted CMGs; at t = 1500 s, two CMGs are failed (i.e., both gimbals are inhibited from selection), and control must be accomplished thereafter via the surviving CMGs and reaction control jets.

Results are shown in Figure 24; gimbal angles are plotted at left. The start of the test is analogous to that of the nominal case (Figure 22) until CMGs #1 and #2 are failed at t = 1500 s. Other CMGs are used extensively to continue nulling the environmental torques until they eventually converge in momentum saturation after t = 3000 s. Attitude control between t = 3000 and 4000 s is achieved primarily via jets; small CMG deflections about saturation are executed to trim these firings. When input requests are directed away from saturation after t = 4000 s, the CMGs are again able to respond to commands and once more provide attitude stabilization (thereby removing themselves from saturation).

FIGURE 24: Hybrid On–Orbit Operation After Two CMG Failures

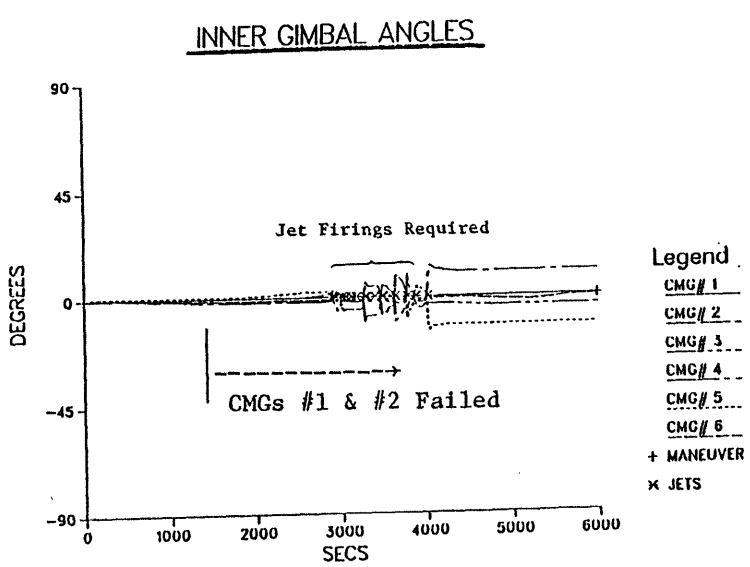

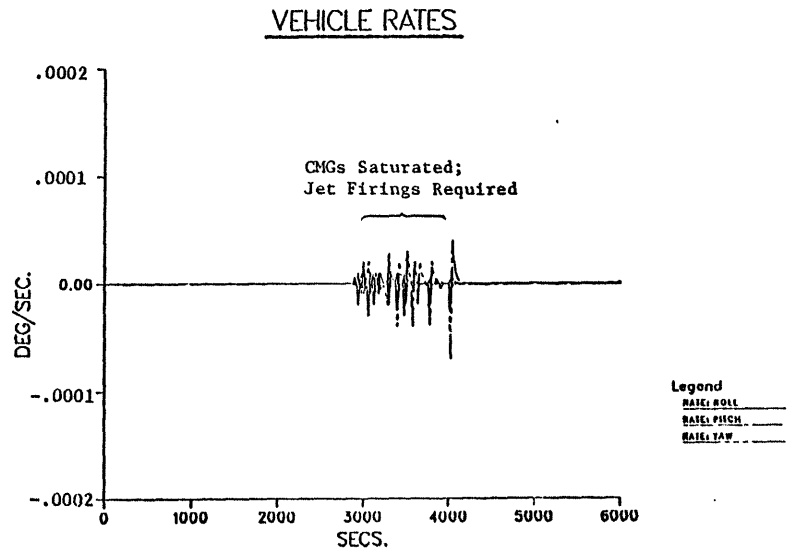

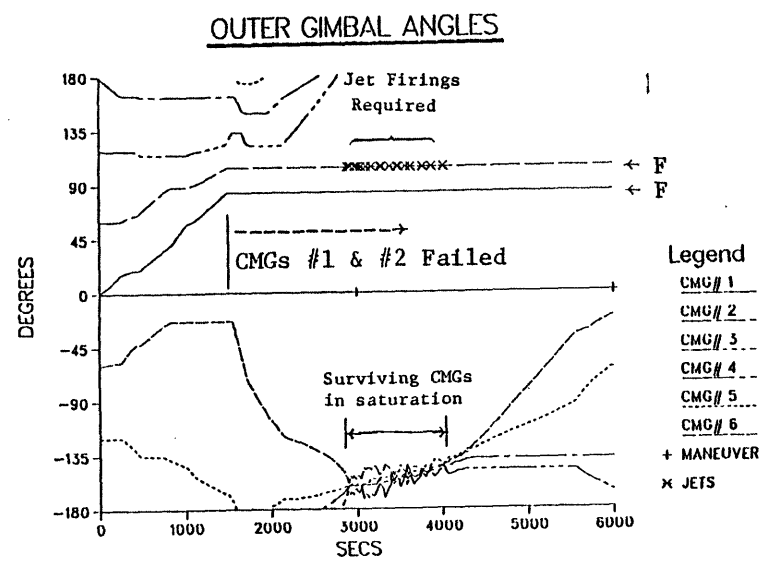

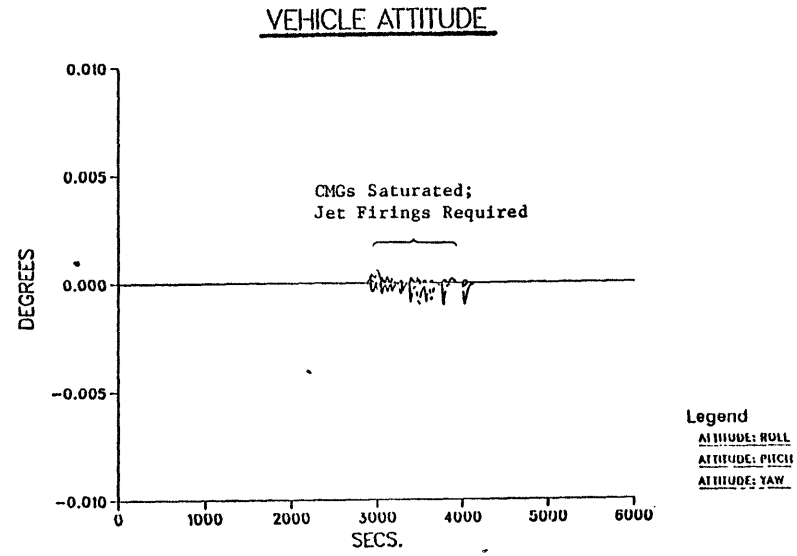

Vehicle rates and attitude are shown in the right column of Figure 24. A higher disturbance level is noted during the region where jets were required (primarily due to their impulsive action and much higher control authority). Vehicle rates were nonetheless maintained within 10^{-4} deg/s, and attitude errors remained negligible.

Example #13: On-Orbit Desaturation of the CMG System

The previous example illustrated how jets were automatically introduced to maintain vehicle control after CMGs were driven into momentum saturation. Another option can be pursued when momentum saturation is detected. Jet firings and CMG motion can be specifically coordinated to desaturate the CMG system (i.e., lower the net stored momentum), enabling continued CMG response to input requests.

The hybrid controller may realize jet desaturation in several ways. The simplest means of achieving a limited desaturation is to merely adjust the CMG vs jet objective factors in hybrid selections, such that extensive "favorable" CMG motion (with respect to a lower objective evaluation) is mixed with jet firings in response to routine requests. Another method, which has been demonstrated with some success, involves enabling both jets and CMGs to be selected simultaneously via the simplex-based null motion process. This will combine favorable CMG motion with jet firings to produce a zero net rate change, thereby driving the CMGs into a minimum-cost configuration and generally achieving significant desaturation. These techniques are demonstrated and discussed at length in Reference 3.

Another more conventional desaturation strategy may also be pursued by firing the jets to apply a momentum impulse to the vehicle equaling the stored CMG momentum, while simultaneously commanding the CMGs to produce an opposing torque. This should ideally return the momentum state of the CMG system to zero.

The example of Figure 25 examines an application of the latter strategy. The Dual Keel model is used with a 6-CMG parallel-mounted configuration (Figure 2). The vehicle is offset from equilibrium by

1.5 degrees in pitch, thus creating an imbalance between averaged gravity gradient and aerodynamic torques which results in considerably increased momentum loading about this axis. The remaining coordinates are aligned with the vehicle principal axes, yielding otherwise reduced environmental torques and smaller Euler coupling.

Inner gimbal angles are shown at upper left. Since the outer gimbals cannot exert a torque about the pitch axis (as mounted in this configuration), significant inner gimbal displacement is required to maintain attitude. As a result, inner gimbal angles increase until momentum saturation is approached when they near 90 degs. At this point, the saturation condition is detected (via the saturation index plotted at upper right), and the desaturation logic sketched above is automatically activated.

The efficiency of this desaturation method is evident in Figure 25; while jets are firing, inner gimbal angles are promptly returned to zero and the saturation index is dramatically decreased. CMGs are then once more able to maintain vehicle attitude until they again load up with momentum, eventually initiating another jet desaturation. This process is repeated as required, creating the observed ramp response in the CMG gimbal angles and saturation index (note that the mean time between desaturations may be reduced in this case by firing jets to load the CMGs with momentum about the axis opposite to the initial saturation). Outer gimbals are used to stabilize the vehicle attitude about roll and yaw; since the vehicle coordinates were adjusted in this example to minimize coupling and environmental torques about these axes, most outer gimbal motion is dedicated to reducing jet-related disturbances and minimizing inner gimbal crosscoupling.

Vehicle attitude is plotted in the lower right corner of Figure 25. Short spikes are seen to develop about the pitch axis during the desaturation intervals. These are due to the mismatch of authority between jets and CMGs; during most of the desaturation process, the CMGs were torque-saturated, allowing the jets to produce a net torque on the vehicle. Incidental vehicle disturbance may be reduced by pursuing a policy that desaturates over longer intervals (i.e.,

FIGURE 25: On–Orbit Desaturation of CMG System

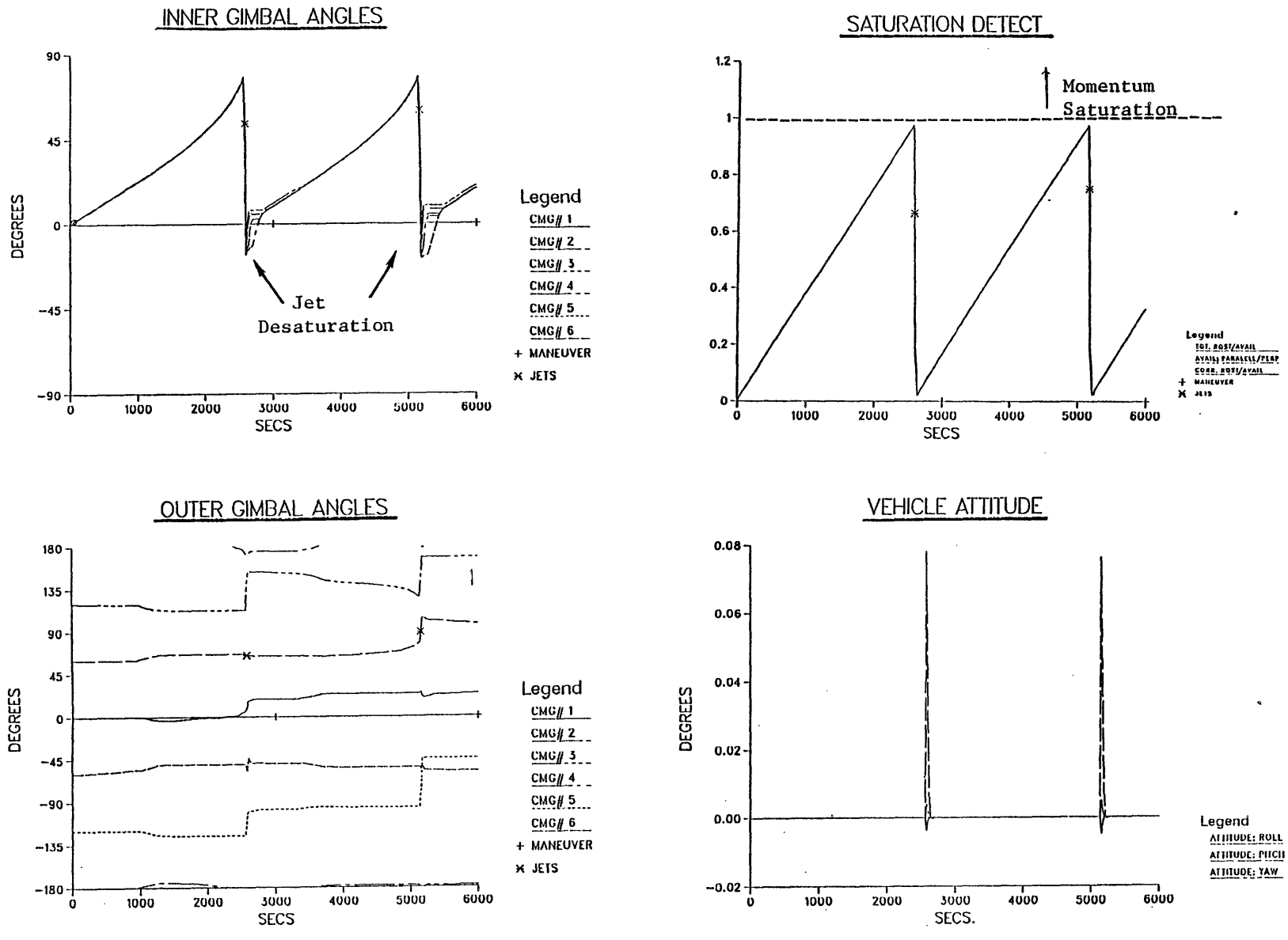

combining several smaller desaturation steps), such as the null motion process discussed in Reference 3.

CONCLUSIONS

Linear programming has been successfully adapted to manage arbitrarily-defined arrays of both CMGs and jets. Closed-loop attitude controllers and environmental models have been developed in order to drive the linear programming selection/steering process and examine its performance under both inertial and on-orbit simulations. The flexibility implicit in linear programming has been seen to enable modes of CMG operation which cannot be achieved with standard (e.g., pseudo-inverse) CMG steering laws. Investigations have also been conducted into the application of linear programming techniques to steering systems of single gimballed CMGs, achieving coordinated translational/rotational vehicle control, and automatically desaturating the CMG system with reaction control jets.

ACKNOWLEDGEMENTS

The author wishes to thank Ed Bergmann, Harvey Malchow, Phil Hattis and Steve Bauer for helpful discussions. The work was prepared at the Charles Stark Draper Laboratory under Independent Research and Development Project #207 and National Aeronautics and Space Administration contract NAS917560.

Publication of this paper does not constitute approval by NASA of the findings or conclusions contained herein. It is published for the exchange and stimulation of ideas.

REFERENCES

(1) Kennel, H.F., "Steering Law For Parallel Mounted Double-Gimballed Control Moment Gyros - Revision A," NASA TM-82390, Jan. 1981.

(2) Paradiso, J.A., "A Highly Adaptable Steering/Selection Procedure for Combined CMG/RCS Spacecraft Control," Proc. of the 1986 American Astronautical Society Rocky Mtn. Guidance & Control Conf., AAS-036, Feb. 1986.

(3) Paradiso, J.A., "A Highly Adaptable Steering/Selection Procedure for Combined CMG/RCS Control; Detailed Report," C.S. Draper Lab, Report CSDL-R-1835, March 1986.

(4) Schiehlen, W.O., "Two Different Approaches for a Control Law of Single Gimbal Control Moment Gyro Systems," NASA TM X-64693, Aug. 2, 1972.

(5) Bradley, S.P., A.C. Hax, T.L. Magnanti, Applied Mathematical Programming, Addison-Wesley Publishing Co., Reading, Mass., 1977.

(6) Paradiso, J.A., "An Efficient OFS-Compatible Kinematic Model for Generalized CMGs," C.S. Draper Lab. Dept. 10C Space Station Memo 85-9, March 25, 1985.

(7) Bergmann, E.V., S.R. Croopnick, J.J. Turkovich, C.C. Work, "An Advanced Spacecraft Autopilot Concept," Journ. of Guidance and Control, Vol. 2, No. 3, May/June 1979, p. 161.

(8) This autopilot was flight-tested on Space Shuttle missions STS 51G (June 1985) and STS 61B (Nov. 1985).

(9) "Space Station Reference Configuration Description," NASA/JSC, JSC-19989, August 1984.

(10) Bishop, Lynda, NASA/JSC-EH, Personal communication, March 5, 1986.

(11) Skylab Program: Operational Data Book, Vols. II and IV, NASA MSC-01549, 1971.

(12) "Space Station Advanced Development Control Moment Gyro (CMG) Data," NASA MSFC memo ED15-85-43, July 1985.

(13) Malchow, Harvey CSDL, Personal communication, July 1986.